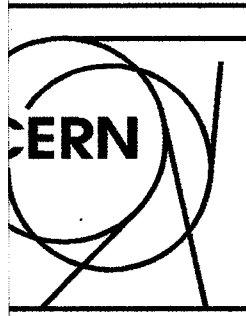


LHC.92.1 3999 0130
0131
0132
0133
0134
0135
0136

Copy 2
J.L. Boldy



ORGANISATION EUROPÉENNE POUR LA RECHERCHE NUCLÉAIRE
EUROPEAN ORGANIZATION FOR NUCLEAR RESEARCH

Laboratoire Européen pour La Physique des Particules
European Laboratory for Particle Physics

LHC CIVIL ENGINEERING CONSULTANCY SERVICES

PACKAGE 02

GEOTECHNICAL INTERPRETATIVE REPORT

DOCUMENT 02/REVISION 1

JULY 1996



N° 818.

DOCUMENT CONTROL SHEET

GIBB-SGI-GEOCONSULT JOINT VENTURE

PROJECT: LHC Civil Engineering Package 02 JOB NO. 96107

TITLE: GEOTECHNICAL INTERPRETATIVE REPORT

ISSUE	DATE
FOR COMMENT	24 May 1996
ORIGINAL	July 1996
REVISION	
REVISION	
REVISION	

This report, and information or advice which it contains, is provided by the Joint Venture in performance of the Joint Venture's duties and liabilities under its contract with CERN. Any advice, opinions or recommendations within this report should be read and relied upon only in the context of the report as whole. The contents of the report do not, in any way, purport to include any manner of legal advice or opinion. This report is prepared in accordance with the terms and conditions of the Joint Venture's contract with CERN. Regard should be had to those terms and conditions when considering and/or placing in any reliance on this report. CERN may release this report to any party having an interest or potential interest in the project. Save therefore, the release by CERN of this report is subject to prior written agreement by the Joint Venture, upon such terms and conditions as shall be agreed upon.

Copies to:

Copy	1	2	3	4	5	6	7	8	9	10
Holder	CERN	CERN	CERN	CERN	CERN	GIBB	GIBB	GIBB	SGI	GC

LHC CIVIL ENGINEERING CONSULTANCY SERVICES

PACKAGE 02

GEOTECHNICAL INTERPRETATIVE REPORT

Chapter	Description	Page
1.	INTRODUCTION	1
	1.1 Project Description	1
	1.2 Terms of Reference	1
	1.3 Data Sources	2
2.	SITE LOCATION AND DESCRIPTION	3
3.	REGIONAL GEOLOGY	4
	3.1 General Geological Setting	4
	3.2 Geological Development of the Geneva Basin	4
	3.3 Structural Geology	6
	3.4 Neotectonics	7
	3.5 Mineralogy of the Molasse Rouge	7
4.	PREVIOUS GEOTECHNICAL INVESTIGATIONS	8
5.	CURRENT GEOTECHNICAL INVESTIGATION	9
6.	DETAILED GEOLOGICAL MODEL	10
	6.1 Introduction	10
	6.2 Geological Materials	10
	6.2.1 Moraine	10
	6.2.2 Molasse	12
	6.3 Detailed Lithological Correlation	15
	6.4 Rockhead Morphology	17
7.	DETAILED GEOTECHNICAL MODEL	18
	7.1 General Methodology	18
	7.2 Geotechnical Units	20

Chapter	Description	Page
8.	HYDROGEOLOGY	24
	8.1 Introduction	24
	8.2 Water Bearing Units	24
	8.3 Hydrogeological Testing	25
	8.3.1 Pump Tests	25
	8.3.2 Borehole Packer (Lugeon) Tests	26
	8.3.4 Piezometer Installations	27
	8.3.5 Flowmeters	29
	8.3.6 Tracer Testing	29
	8.4 Hydraulic Behaviour	30
9.	GEOTECHNICAL CHARACTERISATION	32
	9.1 Moraine	32
	9.1.1 Introduction	32
	9.1.2 Lithological Descriptions	32
	9.1.3 Geotechnical Parameters	32
	9.1.4 In-situ Horizontal Effective Stresses	34
	9.1.5 Foundations for Surface Structures	36
	9.2 Molasse - Time Independent Assessment	37
	9.2.1 Key aspects of Rock Mass Behaviour	37
	9.2.2 Basic Rock Material Properties	38
	9.2.3 Rock Material Strength	39
	9.2.4 Discontinuity Parameters	41
	9.2.5 Summary of Selected Parameters for Molasse for Design	42
	9.2.6 Parameter Uncertainty Assessment	44
	9.3 Molasse - Time Dependant Assessment	44
	9.3.1 Swelling - Fundamental Considerations	44
	9.3.2 Swelling Tests - Particular Observations	46
	9.3.3 Implied Behaviour	48
10.	IN SITU STRESS	50
	10.1 Introduction	50
	10.2 LHC Hydrofracture Stress Measurements	50
11.	ADDITIONAL INVESTIGATIONS	52

REFERENCES

LIST OF FIGURES

Figure No.	Title
2.1	Layout of Underground Structures.
3.1	Regional Geological Map.
3.2	Geological Section through the Geneva Basin.
3.3	Location of earthquake epicentres in the Geneva Region.
3.4	Geologic Timescale.
5.1	Locations of Boreholes and Sections.
6.1	Lithostratigraphic Correlation - Section 1.
6.2	Lithostratigraphic Correlation - Section 2.
6.3	Lithostratigraphic Correlation - Section 3.
7.1	Graph of Depth vs Calliper Log Response.
7.2	Frequency Characteristics of Natural, Tectonised Discontinuities by Lithology Type.
7.3	Combined Lithostratigraphic Correlation and Key Indicators - Section 1.
7.4	Combined Lithostratigraphic Correlation and Key Indicators - Section 2.
7.5	Combined Lithostratigraphic Correlation and Key Indicators - Section 3.
7.6	Composition of a Typical MG Geotechnical Zone.
7.7	Composition of a Typical SS & SW Geotechnical Zone.
7.8	Composition of Typical SM Geotechnical Zones.
9.1	Summary Histograms of Unconfined Compressive Strength.
9.2	Summary Histograms of Tensile Strength.
9.3	Summary Histograms of Deformation Modulus.
9.4	Graphs of Moisture Content and UCS Characteristics for Marl Grumelense.
9.5	Mohr-Coulomb Envelope for Marl Grumelense Peak Strength Triaxial Data (Upper Bound).
9.6	Mohr-Coulomb Envelope for Marl Grumelense Peak Strength Triaxial Data (Lower Bound).
9.7	Mohr-Coulomb Envelope for Weak Marls Peak Strength Triaxial Data.
9.8	Mohr-Coulomb Envelope for Transitional Sandstones and Marls Peak Strength Triaxial Data.

- 9.9 Mohr-Coulomb Envelope for Marl Grumeleuse Residual Strength Triaxial Data.
- 9.10 Mohr-Coulomb Envelope for Marl Residual Strength Triaxial Data.
- 9.11 Barton-Bandis Envelopes for Existing and Incipient Bedding Discontinuities.

1. INTRODUCTION

1.1 Project Description

The Large Hadron Collider project involves the construction of a new machine and associated works, within the existing underground and surface facilities which currently house the Large Electron Positron accelerator (LEP). Additional new structures are required at several locations around the CERN sites. Civil Package 02 encompasses the civil works at Point Five on the LEP ring. A new detector, the Compact Muon Solenoid (CMS), will be installed. This will require the construction of two new caverns, two new shafts, several tunnels and a number of surface buildings of steel and concrete construction.

1.2 Terms of Reference

The Civil Engineering Consultancy Services for Package 02 are provided by the GIBB-SGI-Geoconsult joint venture, in five phases of work. The Phase One preliminary design includes the preparation of this Geotechnical Interpretative Report, using data from a ground investigation Factual Report (GADZ 1996a) prepared by others, a literature review and interviews with local experts (see 1.3 below). The Terms of Reference for this report are:

Sent
with
tender

Prepare and deliver to CERN a geotechnical interpretative which shall include without limitation:

- A review of all geotechnical data supplied by CERN and all other relevant data which ought reasonably to have been obtained from public sources.
- A description of the method adopted to establish the geological model to be used in the numerical analysis.
- A description of the process used to determine the geotechnical parameters for each of the geological units.
- Proposals for additional site investigation work considered imperative for completion and execution of the Works.

The main objective of this report is to provide a geotechnical model and associated geotechnical parameters, to allow design of the surface buildings, shafts and caverns to proceed, such that at the end of Phase One, the layout of the proposed facilities may be frozen and feasible designs may be taken forward to subsequent detailed design phases.

1.3 Data Sources

The following data sources (other than CERN) were used in the preparation of this report:

- A literature review was undertaken to obtain references of direct relevance to underground construction in similar ground conditions. Not surprisingly, this yielded information concerning construction of the LEP project. few other references of direct relevance were obtained. A number of useful papers concerning local and regional geology and geotechnics were also obtained.
- To better understand some aspects of the previous ground investigation and subsequent Factual Report, representative core retrieved from the Point Five site was inspected, accompanied by Jean-François Hotellier, the engineering geologist responsible for the design, supervision and reporting of the ground investigation. His assistance is greatly appreciated.
- Visits to existing underground excavations on the LEP ring were made, to observe rock mass deformation phenomena, and to inspect freshly-retrieved core from horizontal boreholes.
- Valuable information and advice was also supplied by Professor François Descoedres, professor and Director of the Institute for Rock Mechanics at the Swiss Federal Institute of Technology at Lausanne. Professor Descoedres has been involved in the geotechnical aspects of many construction projects in the region, including underground excavations in molasse.
- Discussions with the Geneva Canton Geologist, M. G Amberger, who provided much useful background information on the Geneva Basin.

Data from all these sources were used in the preparation of the first issue of this report. In June 1996, GADZ, as geological and geotechnical investigations consultants to CERN, completed an interpretation of data from the Point Five site (GADZ 1996). This constitutes an additional source of data for revision of this report.

2. SITE LOCATION AND DESCRIPTION

The Point Five site is located some 10 km to the north-northwest of Geneva, near the village of Cessy approximately 3 km from the foot of the Jura mountains. The ground surface lies at an elevation of around 509 m above Sea Level (aSL) and slopes gently to the south-east. The site is crossed by two water courses, to the east and west of the site. A single cavern (HJ56) and shaft (PM56) were constructed at the site as part of the LEP facilities, together with the main LEP tunnel. The beam level at this site is some 420 m aSL, approximately 89 m below ground level (bGL).

The primary proposed facilities consist of the following:

- access shaft PX 56, of oval cross-section with diameters of 21 m and 17 m extending to a depth of approximately 75 m bGL;
- cavern UXC55, which will house the CMS detector, of 53 m length and 26.5 m maximum span;
- access shaft PM54, of 12 m diameter extending to a depth of approximately 80 m bGL; and
- cavern USC55, which will contain the control equipment, and is 85 m in length and 18 m in span.

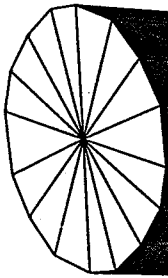
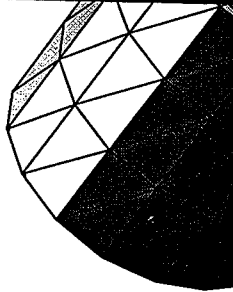
A number of surface buildings are required, both during the assembly of the LHC experimental equipment, and during the operation of the facilities. Of particular significance is a large crane (2500 tonnes capacity), which will require substantial foundations. In addition, erection of the detector will impose large transient loads on the foundations of the principal structures.

Figure 2.1 shows the layout of shafts and underground structures.

PM 54



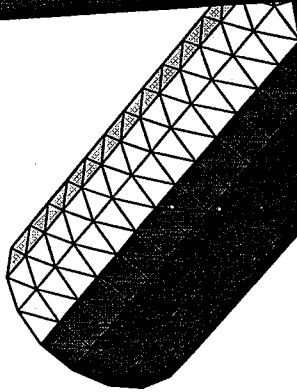
UXC 55



PX 56



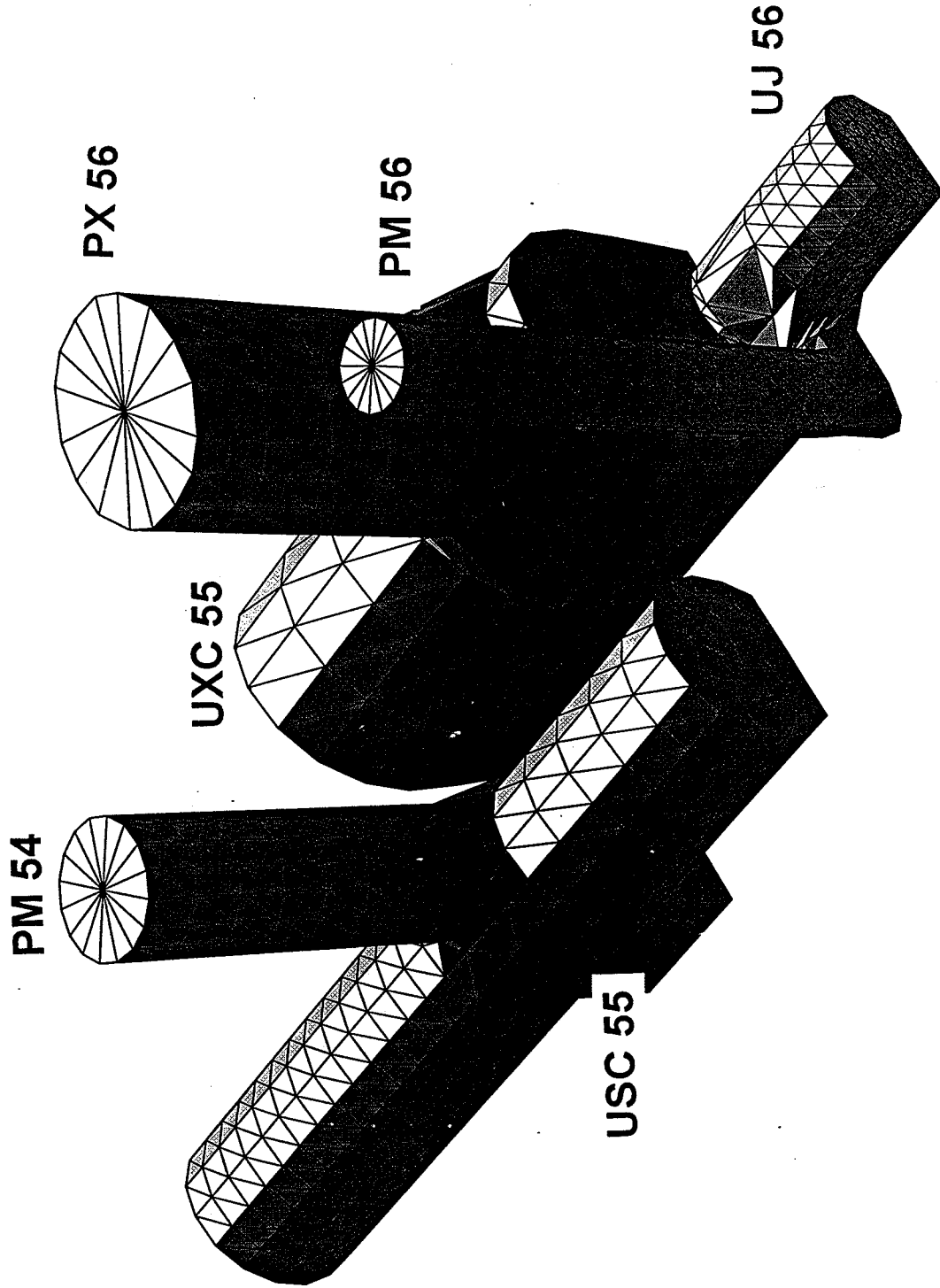
PM 56



USC 55



UJ 56



CERN - LHC PROJECT - POINT 5

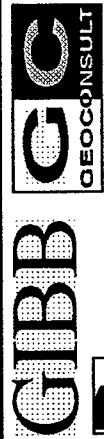
J96107A

Date

JULY
1996

Figure

2.1



3. REGIONAL GEOLOGY

3.1 General Geological Setting

The CERN site is located within the Geneva Basin, a sub-basin of the large North Alpine Foreland (or Molasse) Basin. This is large Basin which extends along the entire Alpine Front from south-eastern France to Bavaria, and is infilled by clastic 'molasse' deposits of Oligocene and Miocene age. The Basin is bounded to the north-west by the Jura mountains, and to the south-east by the Pre-Alps and Alps. The basin is underlain by crystalline basement rocks and formations of Triassic, Jurassic and Cretaceous age. The molasse, comprising an alternating sequence of marls and sandstones (and formations of intermediate compositions) is overlain by Quaternary glacial moraines related to the Würmian and Rissian glaciations. A regional geological map is presented in Figure 3.1.

3.2 Geological Development of the Geneva Basin

The geological characteristics of the molasse and moraine deposits are closely related to the development of the Geneva Basin and to the formation of the Alps. A brief summary of the geological history of the region is therefore described below.

The basement rocks underlying the Western Alps generally comprise crystalline, metamorphosed Palaeozoic sediments, igneous intrusives and extrusives, and Permian-Carboniferous sediments, forming a relatively stable platform area. During the Triassic period, the platform was inundated by a shallow sea, in which deposition of calcareous formations, such as reefal limestones and marls, together with some interbedded scales, were deposited until mid to late Cretaceous times. The style of deposition varied with the depth of the sea, and some periods of intense evaporation led to the formation of gypsum, halite and anhydrite deposits. These evaporites play a critical role in Alpine tectonics. Continental rifting during the Jurassic led to formation of graben and horst structures, with localised sedimentary basins. Upper Cretaceous formations are poorly represented in the Western Alps, as the shallow sea retreated and continental conditions became established through the Eocene epoch.

At the start of the Oligocene epoch, the Alpine Orogeny commenced, and the collision of the African and European continental plates resulted in significant compression across the region, with the resulting formation of the Alps. Major uplift of the Alpine region resulted in widespread erosion of the emerging mountain chain and subsequent deposition in sedimentary basins to the north (Alpine Foreland Basin, including the Geneva Basin), and to the south (Po Basin), of the uplifted area. The sedimentary deposits of these basins are termed 'molasse', and, in the Geneva Basin, comprise a complex, alternating sequence of marls, limestones, sandstones, sandy marls and marly sandstones, deposited in peri-deltaic and shallow marine environments. Up to approximately 3500 m of molasse are believed to have been deposited in the Geneva Basin in the area of Geneva, although the greater part of this sequence has been eroded (Jenny et al 1995). Two major units were deposited; the 'Molasse Rouge' composed principally of marly, silty limestones, sandstones and mottled marls, and the overlying 'Molasse Grise', which comprises marly limestones and marls, with intercalation's of limestones and gypsum (Amberger 1971).

Progressive uplift of the mountain chain resulted in the formation of thrust sheets which are believed to have slid, under the action of gravity, for tens of kilometres along decollement horizons, associated with Triassic evaporite deposits. Such deformations continued throughout the Miocene, and, in the later stage of tectonic activity, resulted in the formation of the Jura mountains. In the Geneva Basin area, the molasse basin itself is believed to have been transported several kilometres on the underlying Triassic evaporates. A cross section through the Geneva Basin is presented in Figure 3.2.

During the Quaternary, the area was affected by two major glaciations; the Rissien and the Wurmien. Ice-sheets up to 400 m thick covered the region, and their migration resulted in significant erosion of the molasse. The Rissien glaciation resulted in the formation of deep (up to 90 m) channels in the eroded upper surface of the molasse. These channels are orientated approximately parallel with the axis of the basin (north-east to south-west), and are understood to have been caused by peri-glacial meltwater flowing from the toe of the ice-sheet. Subsidiary channels also occur, orientated approximately north-south and appear to be related to valleys and major ravines issuing from the Jura mountains. Glacial deposits of Rissien age occur in the floors of these deep channels. These deposits comprise essentially gravels and sands with varying amounts of silt and clay. Some erosion and reworking of these deposits took place during the interglacial period, prior to the commencement of the Wurmien glaciation.

The Würmian glaciation is represented by a sequence of heterogeneous, predominantly granular, moraine deposits. The basal formation comprises the 'Alluvion ancien' which is composed of slightly silty gravel and cobbles, believed to have originated as a fluvial outwash deposit. The overlying deposit is a silty and/or clayey gravel with frequent cobbles. Following the Würmian glaciation, a period of fluvio-glacial deposition occurred as the ice-sheet retreated. These deposits consist of silty and clayey gravels.

For ease of reference, a geologic timescale is shown on Figure 3.4.

3.3 Structural Geology

It is reported that the molasse of the Geneva Basin has been deformed into a number of gentle synclines and anticlines, orientated parallel to the Jura mountains (GADZ 1996). However, structural dips are generally subhorizontal (less than 5 degrees). Recent studies, including seismic exploration and airborne/satellite radar techniques have indicated the existence of major high-angle faults within the molasse (Jenny et al 1995, Charollais and Badoux 1990 and EUROSAT 1982). The strikes of interpreted structural features within the molasse generally fall into four categories (in order of inferred decreasing importance):

1. Faults parallel to the fold axes in the Jura (NNE- SSW).
2. Faults orientated at 345 - 165 degrees (NNW - SSE).
3. Faults orientated approximately perpendicular to the fold axes within the Jura (ESE - WNW).
4. Faults trending east - west.

These orientations generally agree with the orientations of faults mapped within the formations of the Jura and Pre-Alps on either side of the Geneva Basin, and indeed, there appears to be continuity of some of the major features across the complete width of the basin. However, no major faults were located during the construction of the LEP tunnel.

From a consideration of the geological history of the Geneva Basin, it is reasonable to infer the existence of discontinuities within the molasse, especially within the more brittle sandstone units. It would be expected that any discontinuities formed would be sub-parallel to the major structural features, that is steeply-dipping and striking NNE - SSW, E - W, ESE - WNW and NNW - SSE. The scale of such discontinuities may range from major faults of large Aerial extract at spacings of several hundred metres with associated zones of disturbance, to joints of several metres persistence, spaced at some one to five metres.

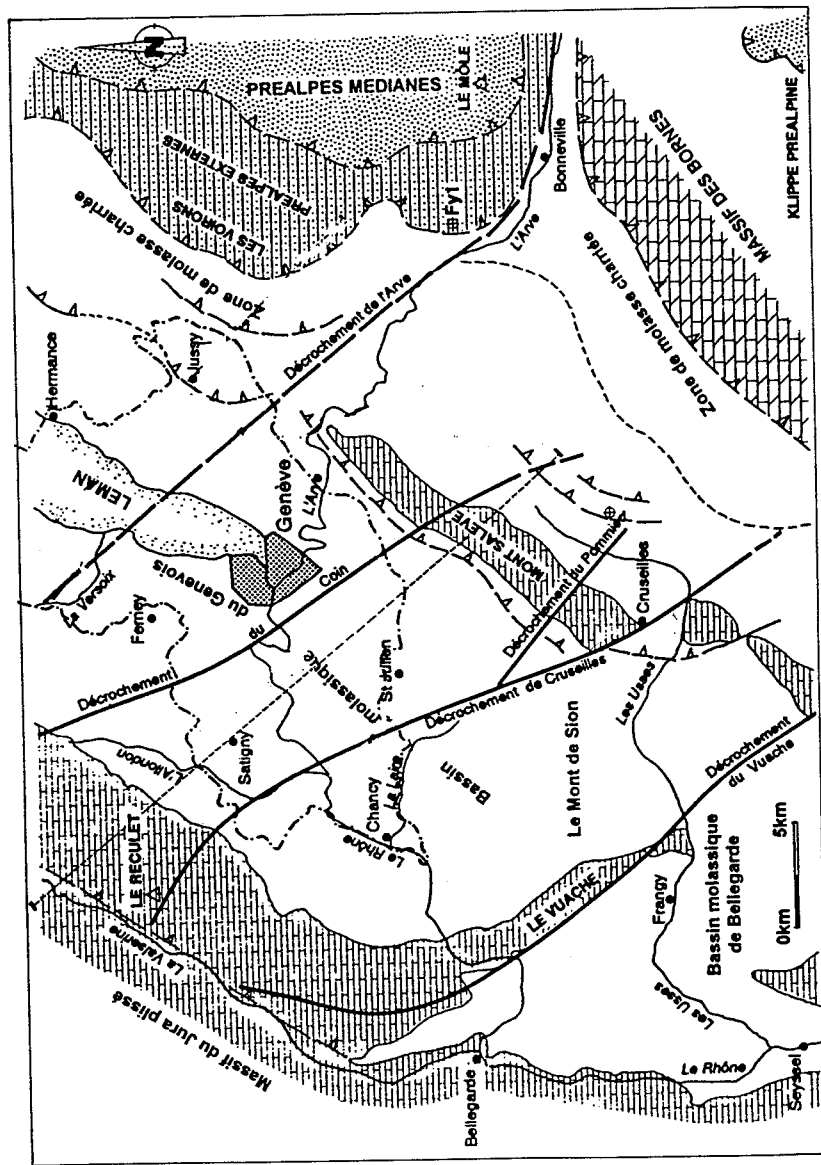
3.4 Neotectonics

The major tectonic event responsible for the formation of the Alps is still active, although it is believed to be in its final stages. Minor seismic events have been noted within South-eastern France and Western Switzerland, and Figure 3.3 presents the distribution of the epicentres. The region is generally considered to be an area of low seismic risk.

3.5 Mineralogy of the Molasse Rouge

The sandstones of the Molasse Rouge Formation generally comprise quartzo-feldspathic micaceous sands, with a calcareous cement. The micaceous component consists of chlorite or muscovite. The grainsize is generally described as 'fine', occasionally 'medium'. In places, the grainsize approaches that of silt (0.002 - 0.06 mm).

In order to investigate the mineralogy of the marls, as part of the current LHC investigation, a number of X-ray diffraction analyses were carried out on the clay fractions obtained from particle size distribution analyses of marl samples. Details of these analyses are given in the Factual Report. Generally, between 40 -55% of the marl samples were composed of clay minerals, with the remainder comprising iron oxides, feldspars, microcrystalline quartz and calcite/dolomite. The majority of the clay minerals are composed of illite, whilst the remainder consist of chlorite and mixed layer illite-smectites. The latter minerals are responsible for the moisture-sensitive behaviour exhibited by the marls.



Legend

Fault Trace

Thrust Fault

Line of Section
(Figure 3.2)

After Jenny et al (1995)

CERN - LHC PROJECT - POINT 5

J96107A

Date

MAY
1996

Figure

3.1

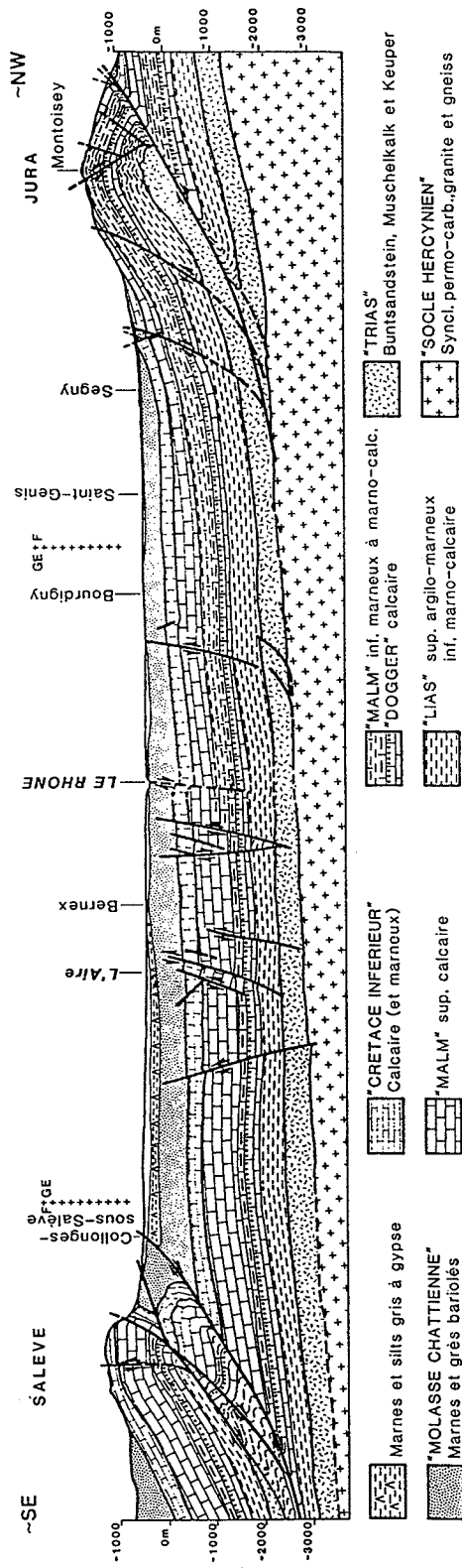
REGIONAL GEOLOGICAL MAP



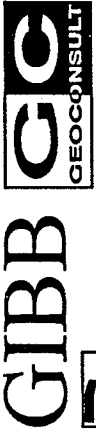

GIBB

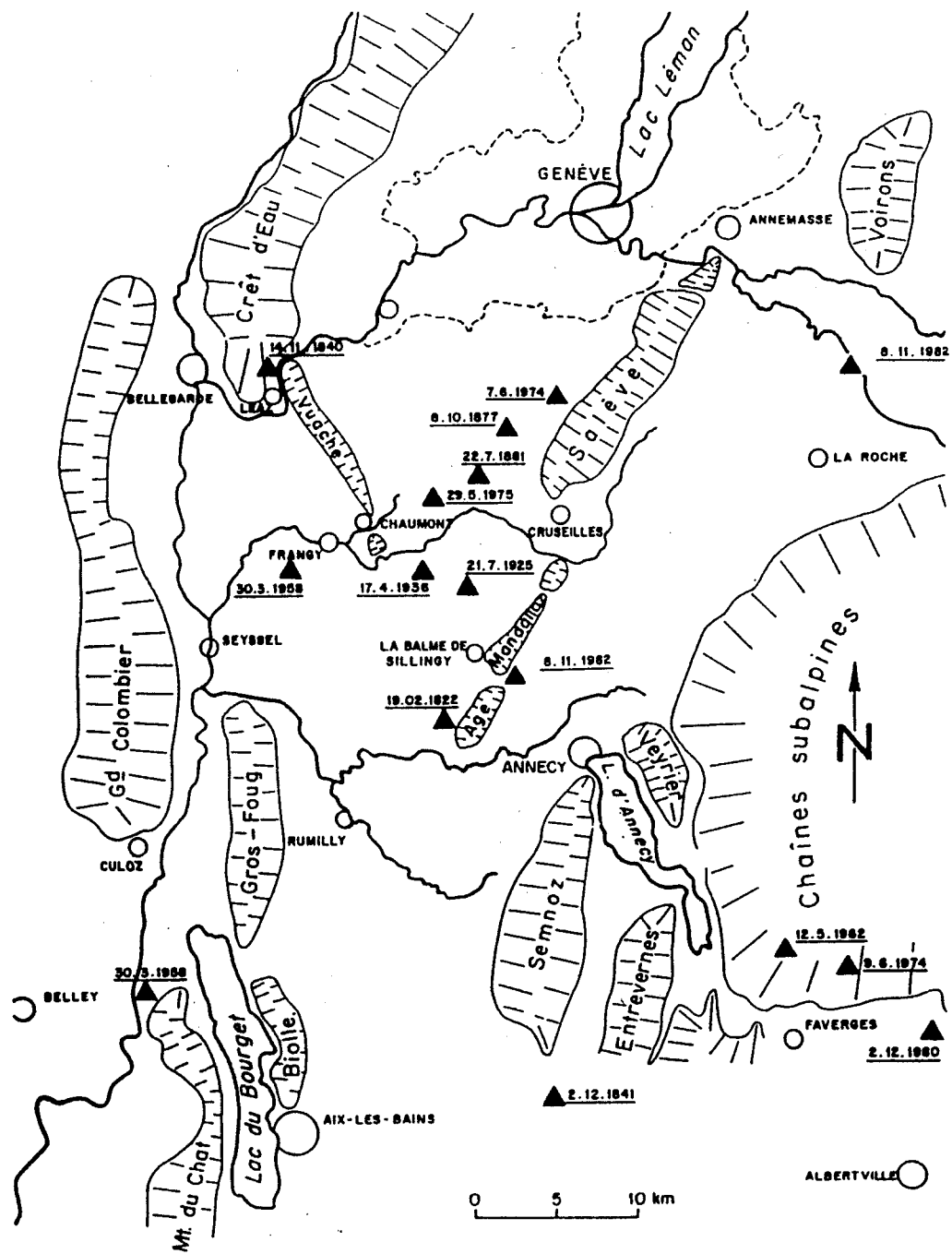


SGE INGENIERIE



Coupe géologique du bassin genevois, entre le Roculet et le chaînon du Salève (Les Pitons) et la Haute-Chaine du Jura. G. AMBERGER (1988).

 	CERN - LHC PROJECT- POINT 5		J96107A
	GEOLOGICAL SECTION THROUGH THE GENEVA BASIN		Date MAY 1996
			Figure 3.2



GIBB



SGI INGENIERIE

CERN - LHC PROJECT- POINT 5

LOCATION OF EARTHQUAKE
EPICENTRES IN GENEVA REGION

J96107A

Date
MAY
1996

Figure
3.3

EON	ERA	SUB-ERA PERIOD		EPOCH	AGE		Abb- rev	Ma	AGE DURATION		
		Quaternary (Q) or Pleistocene (Ptg)	SUB-PERIOD						Ma		
Phanerozoic	Cenozoic	Tertiary	Neogene	Holocene			Hol	0.01	0.01	2.0	
				Pleistocene			Ple	2.0	1.99		
				Miocene	Pliocene	2	Piacenzian		Pia	2.0	3.1
						3.1	Zanclean		Zen	5.1	6.2
							Messinian		Mes	11.3	3.1
						3	Tortonian		Tor	14.4	10.2
							Serravalian		Srv	24.6	8.2
					Oligocene	2	Langhian - Late		Lang2	32.8	5.2
							Langhian - Early		Lang1	38.0	4.0
						1	Burdigalian		Bur	42.0	8.5
			19.5			Aquitanian		Aqt	50.5	4.4	
						Chattian		Cht	54.9	5.3	
			Paleogene	Eocene	2	Rupelian		Rup	60.2	4.8	
					13.4	Priabonian		Prb	65.0	8.0	
						Baronian		Brb	73.0	10.0	
					3	Lutetian		Lut	83.0	4.5	
					16.9	Ypresian		Ypr	87.5	1.0	
				Paleocene	2	Thanetian		Tha	88.5	2.5	
						Danian		Dan	91.0	6.5	
					10.1	Maastrichtian		Maa	97.5	15.5	
					Campanian		Cmp	113	6.0		
					Santonian		San	119	6.0		
		Mesozoic	Cretaceous	K2	Senonian		Coniacian		Con	125	6.0
							Turonian		Tur	131	6.0
							Cenomanian		Cen	144	6.0
							Albian		Alb	150	6.0
							Aptian		Apt	156	7.0
					Early		Barremian		Brm	163	6.0
							Hauterivian		Hau	169	6.0
							Valanginian		Vlg	175	6.0
							Berriasian		Ber	181	7.0
							Tithonian		Tth	188	6.0
				K1	Neocoma		Kimmeridgian		Kim	194	6.0
							Oxfordian		Oxf	200	6.0
							Callovian		Clv	206	7.0
							Bathonian		Bth	213	6.0
							Bajocian		Baj	219	6.0
					Lias		Aalenian		Aal	225	6.0
							Toarcian		Toa	231	6.0
							Phensbachian		Pfb	238	7.0
						Sinemurian		Sin	243	5.0	
						Hettangian		Het	248	1.25	
	Jurassic		J3	Malm		Rhaetian		Rht	253	5.0	
						Norian		Nor	258	2.5	
						Carnian		Crn	263	2.5	
						Ladinian		Lad	268	2.5	
						Anisian		Ans	286	5.0	
			J2	Dogger		Olenekian		Spa	296	1.25	
						Smithian		Smi	315	1.25	
						Dienerian		Die	320	1.25	
						Induan		Gri	333	1.25	
						Tatarian		Tat	352	5.0	
	J1		Lias		Kazanian		Kaz	360	2.5		
					Ufimian		Ufi	367	2.5		
					Kungurian		Kun	374	5.0		
					Artinskian		Art	380	5.0		
					Sakmarian		Sak	387	9.0		
	Triassic		Tr3	Late		Asselian		Ass	268	9.0	
						Gzelian		Gze	286	9.0	
						Kasimovian		Kas	296	9.0	
						Moscovian		Mos	315	9.0	
						Bashkirian		Bsh	320	13.0	
		Tr2	Middle		Serpukhovian		Spk	333	19.0		
					Visean		Vis	352	8.0		
					Tournaisian		Tou	360	7.0		
					Famennian		Fam	367	7.0		
					Frasnian		Frs	374	6.0		
	Tr1	(Early)		Givetian		Giv	380	6.0			
				Eifelian		Eif	387	7.0			
				Emsian		Ems	394	7.0			
				Siegenian		Sig	401	7.0			
				Gedinnian		Ged	408	6.0			
	Permian	P2	Late		Pridoli		Prd	414	6.0		
					Ludlow		Lud	421	7.0		
					Wenlock		Wen	428	7.0		
					Llandovery		Lly	438	10.0		
					Ashgill		Ash	448	10.0		
		P1	Early		Caradoc		Crd	458	10.0		
					Llandeilo		Llo	468	10.0		
					Llanvirn		Lln	478	10.0		
					Arenig		Arg	488	10.0		
					Tremadoc		Tre	505	17.0		
	Carboniferous	C3	Late		Merioneth		Dol	525	10.0		
					20 (Mer)		Mnt	540	10.0		
					St. David's		Men	570	8.0		
					15 (StD)		Sol	570	7.0		
					Caerfai		Len	570	15.0		
		C2	Middle		Attabanian		Atb	570	15.0		
					Tommotian		Tom	590	20.0		
					20 (Mer)		Mnt	525	10.0		
					Maentwrogian		Mnt	525	10.0		
					Menevian		Men	540	8.0		
	Paleozoic	C1	Early		Solvan		Sol	540	7.0		
					Lenian		Len	540	15.0		
					Attabanian		Atb	570	15.0		
					Tommotian		Tom	590	20.0		
					50 (Crf)		Tom	590	20.0		
		C0	Early		Caerfai		Caer	590	15.0		
					Attabanian		Atb	570	15.0		
					Tommotian		Tom	590	20.0		
				50 (Crf)		Tom	590	20.0			
				50 (Crf)		Tom	590	20.0			

GIBB



SGI INGENIERIE

CERN - LHC PROJECT- POINT 5

GEOLOGIC TIMESCALE
(AFTER BRITISH PETROLEUM COMPANY plc 1982)

J96107A

Date
MAY
1996

Figure
3.4

4. PREVIOUS GEOTECHNICAL INVESTIGATIONS

A major geotechnical investigation was carried out prior to the construction of the LEP facilities, including a number of boreholes at the Point Five site. Numerous other engineering projects have been undertaken in the Geneva area, requiring geotechnical investigations. However, as the Point Five site is located in a rural environment, it would appear that no other investigations of relevance have been undertaken in the immediate area.

The LEP investigation, (which was carried out between 1981 and 1982) involved the drilling and testing of numerous boreholes across the Geneva Basin to investigate a number of different alignment options. Boreholes were located along the proposed tunnel alignment, and were also concentrated at the experimental sites. At the Point Five Site, five boreholes were sunk to a maximum depth of 86 m below ground level (bGL), and samples were recovered for subsequent laboratory testing. A limited amount of in situ testing was carried out, comprising packer tests and Standard Penetration Tests. The results of this investigation have been supplied in essentially borehole-specific reports (GADZ 1982a, 1982b and 1982c).

In 1993, during the initial planning stage of the LHC project, a Synthesis Report was completed by Geotechnique Appliqué (GADZ 1993), which summarised all data available from the LEP project. In particular, a large quantity of laboratory test data was analysed, and the results presented as a series of histograms. This provides a useful database against which to compare the results of laboratory test data from the current investigation. However, there are inherent difficulties associated with logging and describing the apparently similar molasse materials, and it is assumed that the logging schemes used in all investigations were consistent.

A significant finding of the LEP investigation was the presence of a buried glacial valley, orientated approximately north-south across the eastern end of the Point Five site.

5. CURRENT GEOTECHNICAL INVESTIGATION

The current investigation for the LHC project commenced in April 1995, with the execution of two boreholes (SLHC14 and 15 to a maximum depth of 51.8 mbGL), primarily to investigate the depth to rockhead.


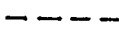
The main investigation phase was carried out between August 1995 and January 1996, and was designed to achieve the following objectives:

- to determine the distribution and characteristics of the various lithologies within the moraine and the molasse, and to investigate the nature of the rockhead surface,
- to determine geotechnical properties,
- to investigate the hydrogeology of the site, especially within the moraine, and
- to investigate the in situ stress regime within the molasse.

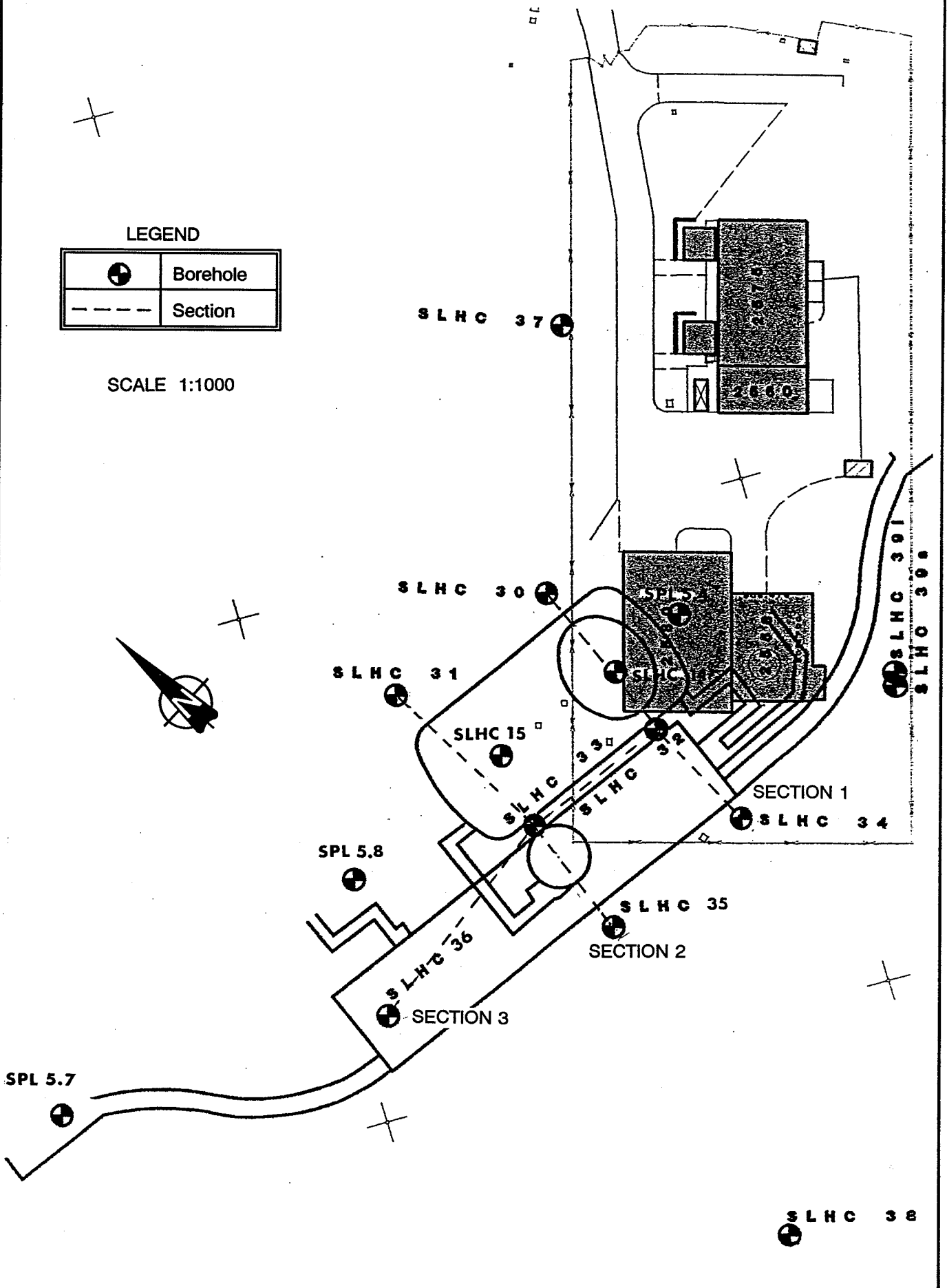
The fieldwork consisted of the drilling and testing of eleven boreholes. The locations of the boreholes are presented on Figure 5.1. Seven boreholes (SLHC 30 - 36) penetrated the molasse to below the proposed cavern depth to investigate the detailed geology for design of the underground investigations, whilst the remaining four boreholes (SLHC 37, 39, 39i and 39s) were sunk within the moraine, preliminary to investigate the hydrogeological characteristics of the site. Laboratory testing of recovered samples to determine geotechnical parameters was carried out at laboratories in France, Switzerland and Italy.

A description of the fieldwork, together with the complete results of the work carried out are fully presented in the Factual Report (GADZ 1996), which also includes a preliminary geotechnical interpretation.

LEGEND

	Borehole
	Section

SCALE 1:1000



GIBB
 **SGI INGENIERIE**

GC
 GEOCONSULT

CERN - LHC PROJECT- POINT 5

BOREHOLE AND SECTION
 LOCATION PLAN

J96107A

Date
 MAY
 1996

Figure
5.1

6. DETAILED GEOLOGICAL MODEL

6.1 Introduction

The derivation of a detailed geological model for the Point Five Site is based primarily upon the data from the boreholes drilled during the 1995 investigation. The main objective of the geological model is to assess the degree of correlation across the site, and to attempt to predict the geological materials which are likely to be encountered in the shafts, caverns and other underground excavations. Such a model is fundamental to the design process, as it forms the framework for understanding the distribution and likely geotechnical properties of the materials across the site. This section of the report describes the general material types encountered at the Point Five Site, the methodology adopted for deriving the detailed geological model, and provides a description of the resulting model.

6.2 Geological Materials

6.2.1 Moraine

The glacial deposits penetrated by the boreholes broadly comprise Wurmien fluvio-glacial deposits, Wurmien boulder/gravel moraine and a fluvial outwash deposit, also of Wurmien age. Moraine of Rissien age which occurs elsewhere in the region is not encountered at this site. Due to extensive excavations within the moraines and previous studies of these materials, a systematic regional lithostratigraphic scheme is well-established, and has been applied at this site during the LHC investigation (GADZ 1996). A degree of interpretation was therefore applied by GADZ during the logging of the boreholes. It should be noted, however, that moraine units are generally very heterogeneous and detailed correlations between even closely-spaced boreholes are sometimes difficult. General qualitative geological descriptions of the materials encountered in the moraines are given below in Table 6.1.

Table 6.1 - Lithostratigraphy of the Moraine

Lithostratigraphic Unit No.	Name and Summary Description
None	Topsoil, Made Ground, Peat
6)	<u>Fluvio-glacial deposits</u>
6a	<u>Sandy gravel</u> Very compact slightly silty sandy gravel, composed of clasts of Jurassic and Alpine rock types. Generally permeable.
6ac)	<u>Silty gravel</u> Compact to very compact sandy gravel in slightly clayey, silty matrix. Gravel is composed of rounded limestone clasts of Jurassic age, generally between 3- 5 cm, occasionally 15- 20 cm maximum dimension. Generally low permeability. Very compact slightly silty sandy gravel. Clasts are rounded and composed of Jurassic and Alpine rock types. Generally permeable.
6b2	Silty fine sand
6c2	Sandy silt
6d2	Silty clayey sand/sandy/clayey silt
7-9	<u>Wurmien Gravel Moraine</u>
7d1)	<u>Silty clayey moraine</u> Very strong massive slightly clayey fine sandy silt with some gravel and occasional boulders. Generally impermeable.
7c1)	<u>Silty moraine</u> Very strong, very dense slightly clayey sandy silt with sandy silty gravel containing many rounded clasts of Alpine rock types, up to 20 cm in size. Generally very low permeability.
7ac)	<u>Silty gravelly moraine</u> Very compact sandy gravel, with matrix of silt with some clay, with clasts composed of Alpine rock types generally 6 - 8 cm in size, but up to 20 cm.
9a)	<u>'Deep stony moraine' (Ancient fluvial outwash deposit)</u> Very compact slightly silty to silty sandy gravel composed of clasts of 5 - 10 cm size, but frequently up to 15 - 20 cm size. Generally permeable, but variable, and with calcareous cemented horizons

Due to the limitations of investigating such a heterogeneous mass with boreholes which yield information which is only truly representative at that point, it is possible that larger boulders than noted above do exist within the moraine.

The major units within the moraine can generally be correlated across the site. However, the borehole logs from the most recent investigation (Borehole LHC 30 to 39) differ significantly from those from previous investigations (Boreholes LHC 14 and 15, and SPL 5.4 to 5.8) as no deposits were interpreted as being of fluvio-glacial origin. Instead, materials within the upper sections of the boreholes are described as single thick units of 9ab) material (Jurassic sand/gravel), with no 6b, 6c, 6d2 material identified. This may be due to differences in the application of the geological logging scheme, or to the fact that these boreholes were executed primarily to determine the depth to rockhead, rather than to investigate the detailed stratigraphy of the moraine.

6.2.2 Molasse

As described in Section 3.0, the molasse comprises a complex, alternating sequence of marls and sandstones, with a range of composite sandy marls and marly sandstones. Individual units vary in thickness between approximately 3.0 m and 0.1 m, and changes in material types are generally gradational. Unlike the moraine, no systematic lithostratigraphic scheme has been developed for the molasse of the Geneva Basin. This is partly due to perceived difficulties in correlating lithologies between boreholes, as a result of lenticularity and facies changes. However, at the Point Five site, a number of marker horizons are present which permit a confident lithostratigraphic correlation to be undertaken, sufficient for detailed design. This is discussed further in Section 6.3. A fundamental, qualitative geological classification of the molasse materials encountered within the boreholes is presented in Table 6.2. The GADZ 1996 Interpretative Report presents a classification of the molasse based essentially upon grainsize and base mechanical properties. This illustrates the gradational nature of the change in grainsize and the corresponding change in mechanical properties. Unconfined compressive strength is used as the index parameter in this classification.

In terms of relative abundance, marls (including marl 'grumeleuse' and 'tectonisée'), sandy marls, marly sandstones and strong sandstones occur approximately equally throughout boreholes drilled within the CERN site. Weak sandstone and limestones are notably less common.

Table 6.2 - Classification of Molasse Lithologies.

Unit	Lithology	Description	Strength	Structure
1.	Limestone	Grey-green/grey occasionally nodular limestone with marl matrix.	Strong	Nodular
2.	Sandstone	Fine grained grey-green, generally grey sandstone,	Strong to very strong	Massive
3.	Sandstone	Fine to medium grained, massive, occasionally poorly cemented grey - green sandstone.	Weak	Generally massive, occasional sub-vertical discontinuities
4a.	Marly Sandstone	Grey-green / grey marly fine sandstone	Strong to very strong	Massive,
4b.	Sandy Marl	Grey-green sandy marl	Strong to very strong	Massive, or thinly bedded
5.	Marl	Dark grey/khaki/grey marl.	Generally moderately strong and strong. Occasionally weak	Thinly bedded or laminated.
6a.	Marl Grumeleuse	Dark grey/khaki/grey/green marl.	Weak to very weak.	Very closely fissured. Fissures are generally randomly orientated with smooth, shiny and striated surfaces.
6b.	Marl 'Tectonisée'	Grey/grey-green or mottled marl.	Weak to very weak	Containing zones of inclined, striated, shiny discontinuities.

6.2.2.1 Marl Grumeleuse

From inspections of core, it is apparent that the marl 'grumeleuse' comprises an element of significant weakness within the rock mass. However, this unit is not discussed at length within the literature, although references are made to materials with 'oblique, close fracturing, the surfaces of which are slicken (sic) and striated' (Laughton 1988). No origin for these units has been postulated, but it is considered that they can be attributed to one or more of the following processes:

- as the molasse thickness was originally of the order of 2,000 m (Jenny et al 1995), most of which has been eroded, the remaining material has been subjected to significant vertical stresses and resultant deviatoric stresses during compaction. These deviatoric stresses (high vertical to horizontal stresses) would have been subject to reversal during erosion, leading to additional, but different, strain patterns. The resulting strains may have been accommodated by fissuring (macroscopic failure) within localised marl units, although it should be noted that not all marl units display the 'grumeleuse' texture.
- Tectonic movements associated with the Alpine Orogeny were ongoing through the Oligocene period, until the Pliocene period. Associated gentle folding and faulting, including thrusts (some of which may have propagated from the basement) may have led to enhancement of strain features and locally, the occurrence of more major zones of shear failure.
- During Quaternary glaciations, ice-sheet thicknesses of over 400 m are believed to have existed within the Geneva Basin. Movement of such glaciers may have induced so-called 'glacial shears' within the low shear strength marl units, giving rise to the highly strained grumeleuse texture. However, it should be noted that the frequency of grumeleuse units shows no decreasing trend with depth, as might be expected

A detailed assessment of the origin of this texture is outside the scope of this Phase One study. The marl grumeleuse, both 'intrinsic' and 'tectonised', are considered to be key geotechnical units in terms of their geotechnical behaviour, and will be identified accordingly in the geological and geotechnical characterisation methodologies.

6.2.2.2 Discontinuity Characteristics

As discussed in Section 3.3, it is reasonable to infer, from the geological history of the Geneva Basin, that although the molasse at the site is generally tectonically undisturbed, discontinuities will exist within some units of the molasse. Such fracturing was noted during construction of underground excavations for the LEP (Laughton 1988), although no detailed orientation data are reported. Laughton reports that the marls contain a significant amount of fracturing, as do weaker, poorly-cemented sandstone units. The transitional materials, the sandy marls and marly sandstones, and the fine-grained sandstones contain only a small amount of oblique and sub-vertical fracturing. Examination of the discontinuity logs from the factual report indicates that the rock mass is locally fractured, with zones of fracture frequencies of 20 - 40%, but occasionally ranging up to 100% (1 fracture per metre).

However it should be noted that these data were acquired from vertical boreholes, which are unfavourably orientated to sample sub-vertical and steeply-inclined features.

However, based upon the available site investigation data and regional geological considerations, it is not expected that significant faulting and associated zones of fracturing will be encountered within the investigation.

6.3 Detailed Lithological Correlation

The lithostratigraphic correlation of the moraine and molasse deposits has been conducted along the following cross-sections, which are based on the data recorded on three borehole logs along each section.

Section 1.	Boreholes SLHC 30, 32 and 34
Section 2.	Boreholes SLHC 31, 33 and 35
Section 3.	Boreholes SLHC 36, 33 and 32

Moraine was proved in all the boreholes to depths between 43.1m (Borehole SLHC 38) and 50.6m (Boreholes SLHC 30 and 37). The elevation of the base of the stratum varied between 456.6m and 463.55m. The moraine is generally described as a very dense silty, sandy and clayey GRAVEL, with cobbles and boulders and occasional bands of silty sandy clay. The clay bands are most numerous within the top 5m of the stratum and appear to reduce in frequency, with depth. As described in Section 6.2.1 a detailed lithostratigraphic classification exists for the moraine and was applied during logging. A broad correlation across the site is therefore relatively straightforward, as shown on Figures 6.1 to 6.3.

All boreholes, except SLHC 37, show the silty, sandy clay bands (6d2 & 6c2) within the top 5m to be up to 1.3m thick, overlain by a cover of very dense silty, clayey gravel, (back) approximately 3m thick. In the case of Borehole SLHC 37, this gravel cover appears to be absent. Instead, the top 5m comprises firm to stiff clay of low plasticity, with occasional bands of clayey gravel. It should be noted that SLHC 37 is set apart some 50m north east of the remainder the group, and would appear to indicate a change in ground conditions in the vicinity of this borehole.

According to the published geological literature (Charollais & Badonx 1990) dips within the molasse of the Geneva Basin are generally at about 5°-10°, which indicates that bedding inclinations should not exceed 10° when correlating boreholes. In spite of an apparent lack of prior systematic correlation of any of the CERN data. Several calcareous horizons were identified, which although subordinate within the overall stratigraphic sequence, can be regarded as primary marker horizons in correlating boreholes. These horizons are identified as C1, C2 and C3 in ascending order. The lower and upper horizons, C1 and C3, respectively, are represented in all boreholes, except horizon C1 in Borehole SLHC34. The middle horizon, C2 is apparently confined to Boreholes SLHC 31 and 35. The correlation of these calcareous horizons between boreholes establishes the structural orientation for correlating the entire stratigraphic sequence.

Sandstones represent secondary marker horizons and have been subdivided into units S1 to S13 in ascending stratigraphic order. These units are not present in all boreholes and in some cases are amalgamated. The sandstones are also laterally persistent, and can be correlated between boreholes to provide additional confidence in the correlations. Some sandstones vary in composition according to the descriptions on the borehole logs. These anomalies may be due to facies changes within a depositional environment characterised by fluctuating energy conditions.

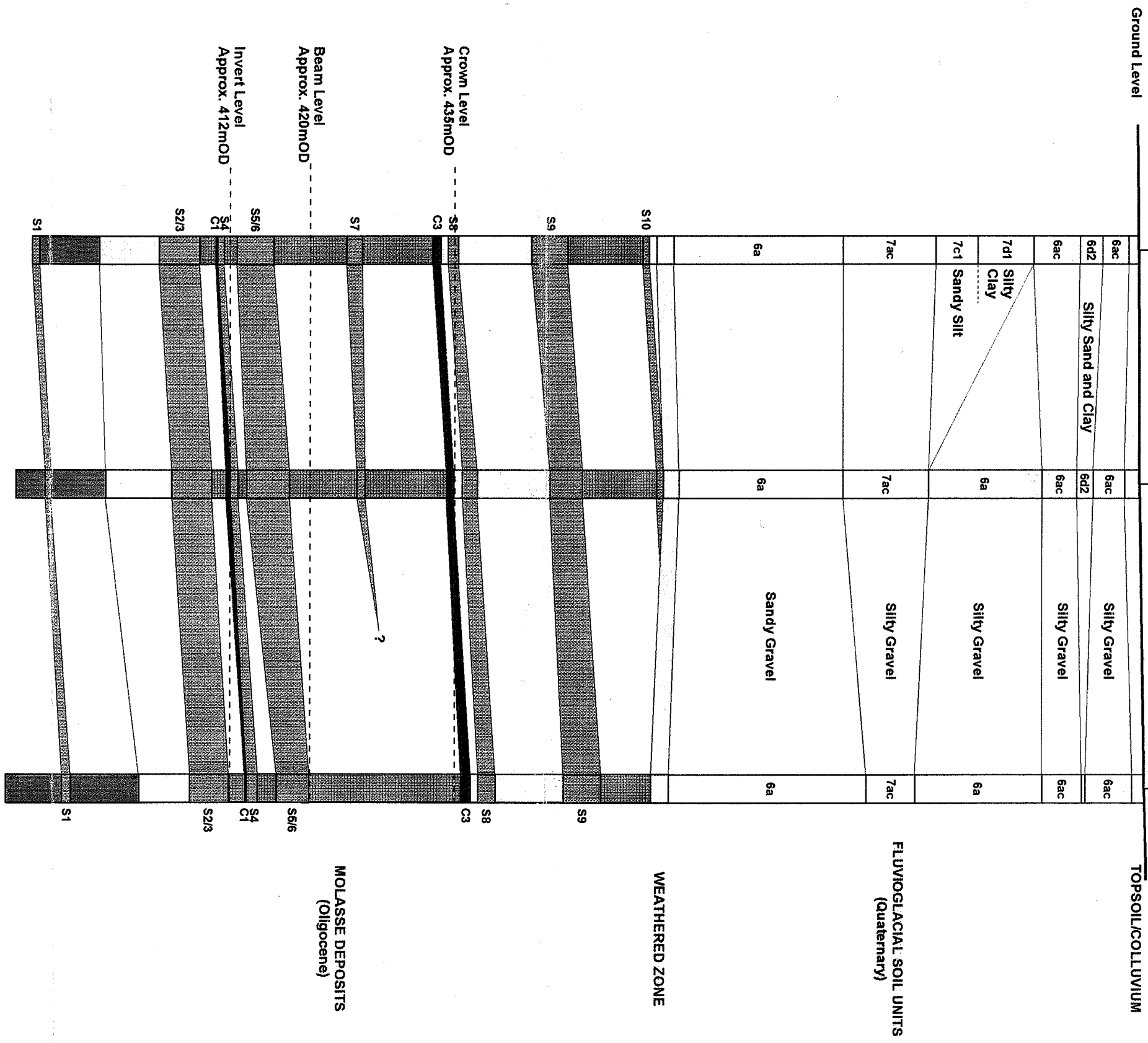
The lithological sequences presented on the borehole logs have been simplified in order to establish a meaningful correlation for engineering purposes, across the site, as shown on Figures 6.1 to 6.3. In particular, units of similar character such as sandy marl and marly sandstone sequences, have been grouped together, and have been correlated across the site.

The marl-dominated deposits in particular exhibit a broad correlation between boreholes. These finer grained deposits include fissured ('grumeleuse') and more sheared ('tectonisee') units, which are identified in the lithological descriptions. These disturbed zones occur throughout the molasse deposits but are relatively more abundant in the marl dominated composite units. As these disturbed zones are generally limited to materials characterised by higher clay contents and may be generally correlated between adjacent boreholes, they are interpreted to be concordant with material boundaries rather than cross-cutting the stratigraphic sequence.

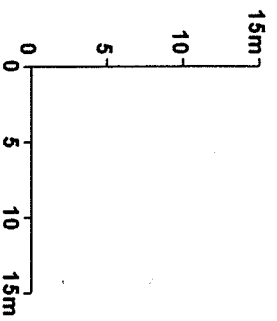
The correlation of boreholes indicates that strata along Sections 1 and 2 (Figures 6.1 and 6.2) dip at about 3° towards the south and at about the same inclination westwards along Section 3. This gives a true dip of approximately 5° to the south - south-west.

6.4 Rockhead Morphology

The Synthesis Report (GADZ 1993) briefly describes the morphology of the surface of the molasse. The Geneva Basin was subjected to deep erosion at the end of the Tertiary period due to widespread glacial and fluvial processes, resulting in a very uneven rockhead surface. Deep channels were scoured by glacial rivers, in places up to 100 m deep, orientated approximately parallel to the basin axis (north-east - south-west), with secondary channels orientated approximately north-south. A rockhead contour map has been produced by the Canton Geological Service (Service Cantonal de Geologie), and shows the distribution of scour channels and ridges. This is based upon data from agricultural wells and other boreholes, principally investigation boreholes for the LEP, but does not include data from the LHC investigation. At the Point Five site, the map indicates a minor channel passing across the site from north to south. This is confirmed by the LHC boreholes, which indicate a minimum rockhead level of 457 m aSL in Borehole LHC 39s, compared with levels of approximately 470 m and 463 m to the east and west of the site, respectively. The channel axis appears to run to the east of the proposed new shaft PX56, as shown on a detailed contour plot of rockhead surface, on Figure 6.4.

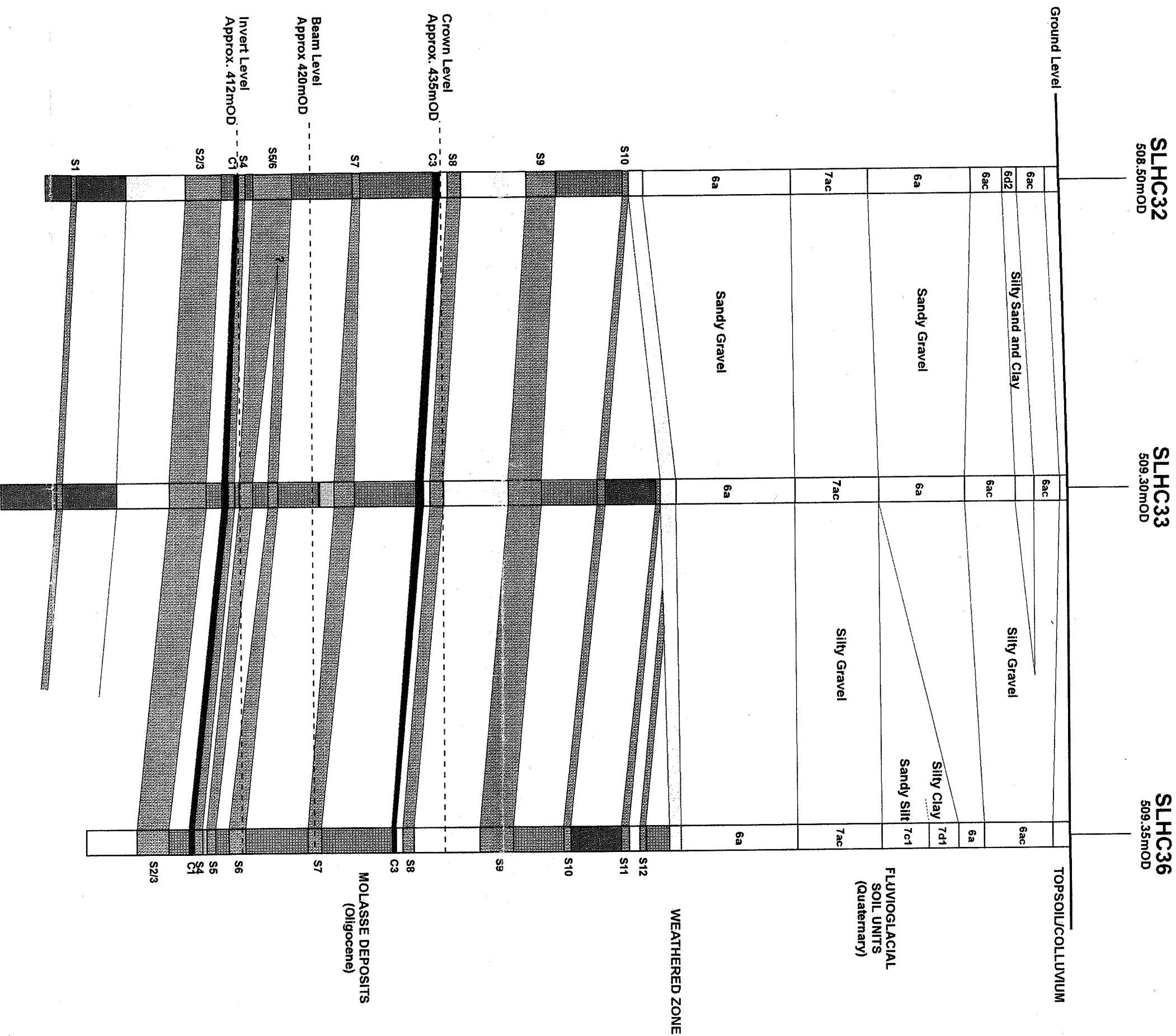


SCALE

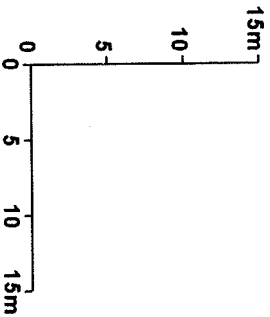


KEY

- Primary Lithostratigraphic Markers
- Secondary Lithostratigraphic Markers
- Composite Units
- C1 and C3 Calcareous Horizons
- S1 - S10 Sandstone Horizons
- Marly Sandstones and Sandstones with Subordinate Marls
- Interbedded Marls and Sandy Marls
- Marls with Subordinate Sandy Marls



SCALE



KEY

- Primary Lithostratigraphic Markers
- Secondary Lithostratigraphic Markers
- Composite Units
- C1 - C3 Calcareous Horizons
- S1 - S12 Sandstone Horizons
- Marly Sandstones and Sandstones with Subordinate Marls
- Interbedded Marls and Sandy Marls
- Marls with Subordinate Sandy Marls

7. DETAILED GEOTECHNICAL MODEL

7.1 General Methodology

From a study of geotechnical data previously acquired and evaluated for the LEP project (GADZ 1993), it is apparent that the major control on the distribution of geotechnical parameters is the stratigraphy of the site. A limited thickness of weathered rock is present at the upper surface of the molasse, but beyond this, there would appear to be no purely depth-related variations in geotechnical parameters. (The controlling effect of stratigraphy is also illustrated in a geomechanical sense by observations both during and after construction of the LEP facilities, where minor rock mass failures were observed to be limited to particular lithologies (pers comm JF Hotellier)). It was therefore considered both reasonable and appropriate to base the detailed geotechnical model on the established lithostratigraphic-stratigraphic correlation for this site, as described in Section 6.0.

However, it is recognised that the lithological marker horizons within the molasse used to establish the correlation are not necessarily the most significant in terms of the geomechanical behaviour of large underground openings. From a consideration of likely strength and deformability characteristics, it is the weaker lithologies, such as the marl grumeleuse and marl tectonisée, as well as the poorly cemented sandstones, which are likely to influence the overall behaviour of the rock mass. Consequently, it is necessary to subdivide the composite units in order to correlate units of similar geotechnical character across the site. However, there is an increased level of uncertainty associated with such a subdivision, due to inherent variations in lithology and lenticularity of individual sedimentological units, but it is essential that the weaker units within the rock mass are characterised in terms of their occurrence and their actual geotechnical properties, with a true representation of contrast.

The following datasets were used as a basis to subdivide the composite units:

1. **Geological descriptions.**

The geological descriptions given in the borehole logs (GADZ 1996) obviously form the primary dataset for any lithological correlation. However, the various marls and sandy marls are of generally uniform appearance, and it is possible that not all sub-units will have been identified during logging. Other indicators are therefore useful as additional data sources.

2. **Geophysical wireline calliper logs.**

As noted in the Factual Report (GADZ 1996) there is a very strong correlation between areas of borehole enlargement and the occurrence of marl grumeleuse. Given the relatively uniform appearance in the core of the various marls and sandy marls and intrinsic difficulty of visual differentiation, the calliper logs provide a large useful index data set to predict the likely occurrence of marl grumeleuse. The signature is generated by the sensitivity of these particular materials to strain release in the borehole wall and moisture sensitivity (softening and slaking).

The calliper logs for Boreholes LHC 30 to 36 were analysed, and the calliper responses broadly classified according to depth of washout and vertical extent. It was considered that a more rigorous classification was not appropriate due to the variable effects of drilling history of the depth of washout features. Comparison of the calliper logs with the lithological descriptions confirmed the validity of the geological correlation. A typical depth profile of calliper responses is presented on Figure 7.1.

3. **Sonic velocity measurements.**

During logging of the core, a large number of sonic velocity measurements was obtained using PUNDIT equipment. These measurements were made to confirm the visual assessment of rock material strength via a general correlation between uniaxial compressive strength and seismic velocity established during the LEP investigation. This broad correlation is shown on Figure 7.2, extracted from the Factual Report. This technique confirms the occurrence of weak sandstones and marl grumeleuse, and increases confidence in the visual assessments of rock material strength. Histograms of seismic velocity for each rock material type are presented in the GADZ Interpretative Report (1996b).

4. **Discontinuity data.**

Detailed discontinuity logs were prepared during core logging, as described in the Factual Report. As part of this study, these logs have been transferred to a database to allow the data to be manipulated. Detailed discontinuity characteristics, such as origin, joint surface morphology, and planarity, were recorded, and allow detailed data assessments to be carried out (see Section 7.2 below).

7.2 Geotechnical Units

Of particular relevance to rock mass strength and deformability, is the occurrence of natural (as opposed to drilling-induced) discontinuities, especially those showing evidence of tectonisation (e.g. slickensides). Histograms showing the total numbers of inclined, natural discontinuities and their frequency characteristics for each major lithology are given on Figure 7.2. Figure 7.2a shows that most fracturing occurs within the marl grumeleuse, as would be expected. A significant number of discontinuities also occur within the sandy marl and marly sandstone units, but detailed examination of the borehole logs shows that fracturing is concentrated within thin marl grumeleuse interbeds.

The sandstones (including both weak and strong rock materials) show a significantly lower degree of fracturing. Figure 7.2b presents a graph of average fracture frequency for each of the three broad lithologies, which takes into account the actual length of each unit cored in the boreholes. This confirms the marked difference in fracture state between the units, with average fracture frequencies of 2.6 per metre, 1.1 per metre and 0.7 per metre for marl grumeleuse, sandy marl and sandstone respectively.

The overall methodology has therefore been to subdivide the geological model, to define and correlate discrete groups (or geotechnical units) of strata of similar geotechnical character, based upon examination of index datasets and then to assign geotechnical parameters to these groups (Section 9).

Figures 7.3 to 7.5 show depth frequency graphs for natural discontinuities and graphs showing the occurrence of various classes of calliper log responses, overlain on the detailed geological model for the Point Five site. The figures clearly show the good correlation between concentrations of discontinuities and the occurrence of marl grumeleuse units, indicated by the calliper logs. It can also be seen that groups of calliper log responses can be broadly correlated between boreholes. However, the correlation becomes more problematic when individual responses are traced across the site. In order to reduce uncertainty therefore, whilst still retaining an appropriate level of detail, marl grumeleuse beds were grouped together into units which were correlated across the site. Similarly, although individual sandstone beds can often be correlated between two adjacent boreholes, sometimes the correlation breaks down over greater distances. However, sandstone beds sometimes occur in groups, which can be correlated with more success.

The following geotechnical units were therefore defined:

1. **Marl Grumeleuse (MG) Geotechnical Unit**

Units were defined based upon approximate linear occurrence of marl grumeleuse rock material within the core. Thus, these units may contain some thinly bedded marls or sandy marls, but overall, the character of the unit is controlled by marl grumeleuse rock material. In general, an individual marl grumeleuse unit is defined if the bed thickness exceeds 0.5 m or if the proportion of marl grumeleuse within a sequence of strata exceeds approximately 40 %. Figure 7.6 contains an extract from Borehole LHC34 showing the composition of a typical MG unit. The unit contains approximately 46% marl grumeleuse material, according to the lithological description, which is considered to be sufficient to control the behaviour of the unit. Where unit thickness is less than 0.5 m, and if the unit can be correlated between boreholes, a separate marl grumeleuse interface is defined. Geomechanical parameters can be defined, and such features can be modelled explicitly in subsequent design work.

2. **Marl (Laminated) (ML) Geotechnical Unit**

These units comprise beds of marl which is generally laminated or thinly bedded and does not exhibit the characteristic grumeleuse texture. The difference in mechanical properties between marl grumeleuse, marl and sandy marl is illustrated by the histograms of sonic velocity and point load strength presented in the GADZ Interpretative Report (1996). Similar distribution of laboratory test data, for UCS or Young's Modulus for example, are difficult to derive due to the limited number of tests. However, the index tests adequately indicate the fundamentally different characters of this material, compared with other rock types. Generally, separate ML zones are defined when bed thickness exceeds approximately 1.50 m. In other instances, thinner beds of marl will be incorporated into SM and MG units, as described in (1) and (5).

3. **Sandstone (Weak) (SW) Geotechnical Units**

These units are limited in number and are selected on the basis of the lithological description, where an assessment of strength has been made visually, and confirmed by PUNDIT sonic velocity measurements. The units generally comprise single beds of weak sandstone which correlate across the site.

4. **Sandstone (Strong) (SS) Geotechnical Units**

These units generally consist of single thick beds of sandstones, which have been described as 'strong' or 'very strong' in the lithological (core logging) descriptions. Alternatively, where thinner such beds are closely spaced, they have generally been amalgamated to form single geotechnical units which may also contain marly sandstones separating well-defined sandstone beds. An example of SW and SS units is given in Figure 7.7, from Borehole LHC33 at 101.65 m depth. This shows an SS unit, including a thin marl bed, above an SW unit.

5. **Sandy Marl (SM) Geotechnical Units**

These units contain materials which are intermediate between marls and sandstones (except where marly sandstones have been incorporated into SS units). They are therefore composite units which may also contain beds of intact (non-grumeleuse) marls. It is considered that these units will not play as critical a role in the behaviour of the rock mass as the marl grumeleuse material, and therefore, such a grouping is reasonable. Where thin (generally less than 0.5 m) marl grumeleuse units occurring within an SM unit can be correlated between boreholes, they are defined as MG interfaces. An example SM unit from Borehole LHC36 to 90.8 m depth is shown as Figure 7.8.

6. **Interface Units**

As described in (5) above, where thin marl grumeleuse units occur, generally less than 0.5 m in thickness, these are defined as 'interface' units, with geotechnical parameters assigned accordingly, these are termed 'mgi'. Similarly, at boundaries between units, where there is likely to a difference in the mechanical response of the rock materials, boundary interfaces are also defined. These are termed 'mgb' for boundaries with marl grumeleuse.

Following definition of these Geotechnical units, correlation throughout the site was carried out, using the three key sections, as shown on Figures 7.9 to 7.11. Generally, the correlations are good, although inevitably, there are some areas of uncertainty and non-continuity. These are interpreted to be a result of lenticularity of some beds, particularly the sandstone units, as would be expected in a fluvial sedimentary environment.

Table 7.1 shows the depths of all boundaries and units for each borehole across the site.

Table 7.1 Geotechnical Zonation for the Point Five Site

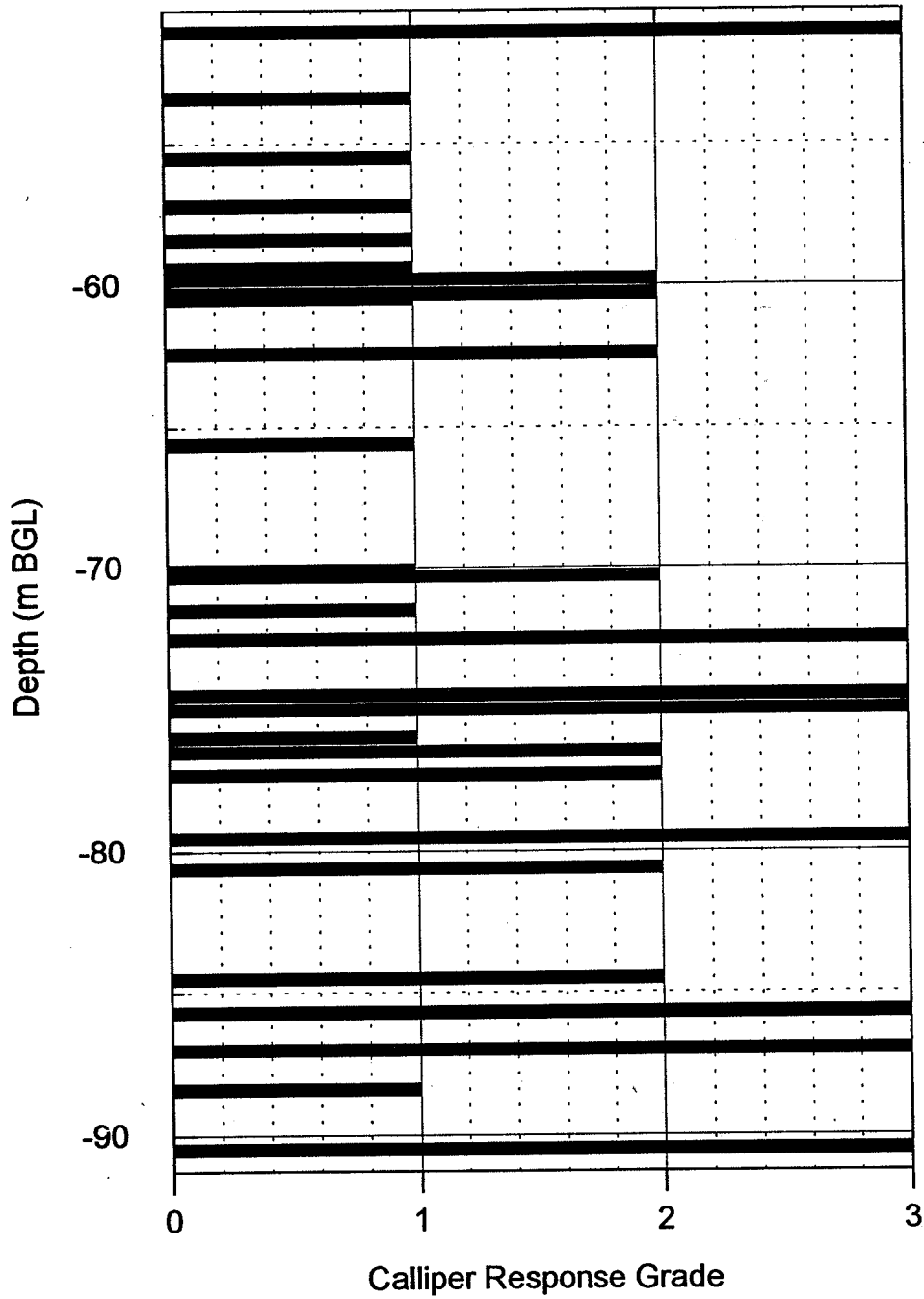
All depths in metres above datum

Lithostratigraphic Unit (Formation Tops)	Borehole No.						
	30	31	32	33	34	35	36
Rockhead	458.4	462.35	459.5	463.2	458.9	463.15	463.55
SM9	nr	460.75	508.5	461.3	457.1	461.15	462.15
S10 (mgb)	nr	457.05	457.8	454.8	456.3	452.95	450.45
SM8 (mgb)	456.5	456	455.5	453.85	455.6	451.7	449.6
	mgi	454.9	454.7	454.2	452.2	450.25	448.55
	mgi	454.35	453.3	453.05	451.5	449.2	447.25
	mgi	453.6	453.05	451.3	449.9	450.4	447.85
S9 (mgb)	451.95	449.9	449.2	447.7	447.6	445.4	443.65
ML3 (mgb)	447.15	445.45	445.7	443.3	443.7	441	439.65
MG7 (mgb)	445.45	443.85	444.5	441.3	442.7	439.85	437.9
	mgi	443.5	442.85	442.5	440.3	442	437.45
ML2 (mgb)	442	440.45	440.3	438.8	438.7	435.55	434.4
S8 (mgb)	439.85	437.75	437.9	435.6	436.4	433.4	431.85
	mgi	437.8	436.35	436.3	434	434.8	431.6
SM7	435.5	434.25	433.6	431.9	432.4	430.25	429.25
	mgi	432.4	431.15	431.15	428.7	429.75	426.65
MG6	430.6	428.9	428.95	426.6	427.6	424.45	425.05
SM6	429.8	428.45	427.85	425.95	426.6	423.65	422.15
S7	nr	427.05	426	425.1	425.7	423.05	420.95
MG5	427	425	424.95	422.7	423.75	421.05	419.05
SM5	426	424.55	424.2	422.1	423.15	420.45	418.55
	mgi	425	421.35	421.75	419.15	420.9	417.85
	mgi	423.5	419.65	421.2	417.2	417.3	415.5
S6 (mgb)	420.05	419	417.95	416.05	416.3	414.55	412.05
	mgi	nr	416.75	nr	414.9	nr	413.3
MG4	nr	416.25	nr	413.9	nr	412.55	nr
S4/5	Incl in S6	415.65	Incl in S6	413.1	Incl in S6	411.75	408.5
SM4	413.4	412.15	411.2	410.2	410.3	407.8	405.95
S2/3 (mgb)	411.5	409.9	409.7	407.65	408.4	406.05	403
ML1	407.4	405.75	405	403.3	404.1	401.8	399.25
SM3	402.2	399.1	399.9	397.15	398.55	395.25	509.35
MG2	398.6	398.05	396.3	396	396.9	394.3	509.35
SM2	396.8	396.1	395.55	393.8	393.2	np	
MG1	396	394.35	394.3	392.35	392.8	np	
SM1	394.85	392.85	392.75	390.8	391.5	np	

nr = not represented
np = not penetrated

MG1 – Marl (Grumeleuse) Unit 1
SM1 – Sandy Marl Unit 1
ML1 – Marl (Laminated) Unit 1
S1 – Sandstone Unit 1
mgb – marl grumeleuse boundary
mgi – marl grumeleuse interface

BOREHOLE SLHC 36



GRADE	DEFINITION
1	Small diameter variation
2	Medium diameter variation
3	Large diameter variation

Figure 7.2a

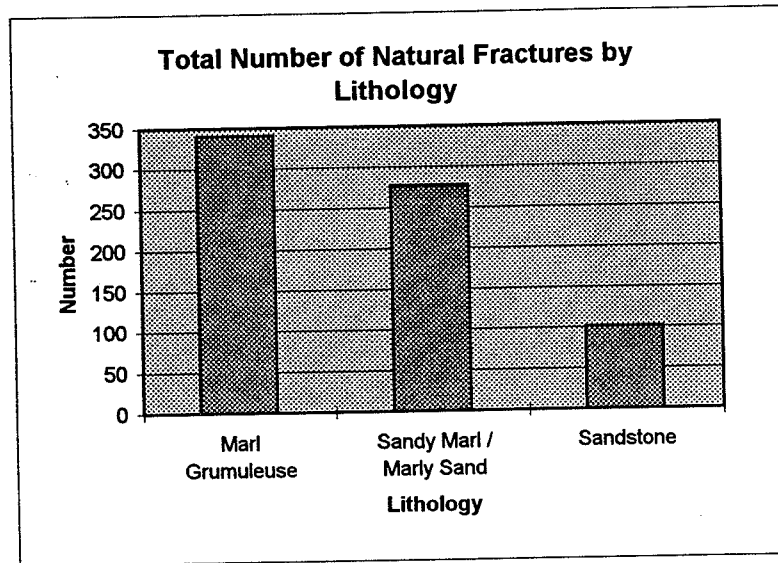
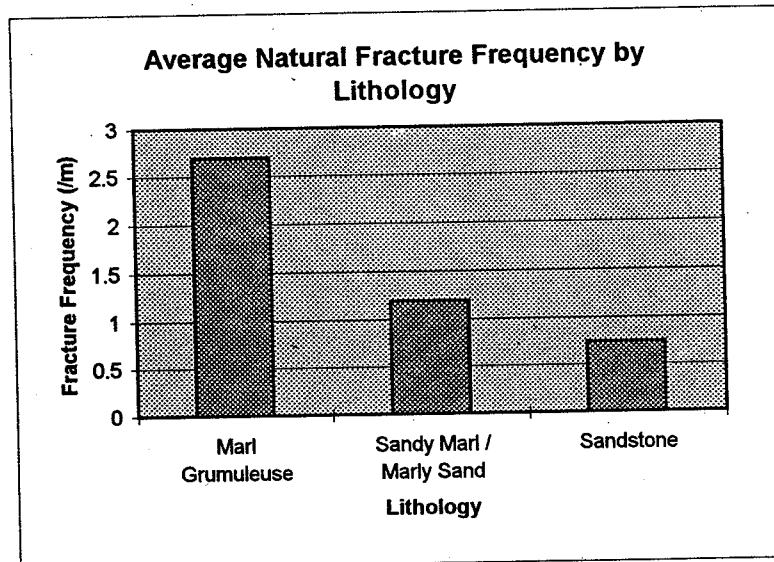


Figure 7.2b



GIBB



SGI INGENIERIE



CERN - LHC PROJECT- POINT 5

FREQUENCY CHARACTERISTICS OF
NATURAL TECTONISED DISCONTINUITIES
BY LITHOLOGY TYPE

J96107A

Date
MAY
1996

Figure
7.2

Extract from Borehole SLHC 34 log

Depth (m BGL)	Geotechnical Unit	Legend
102.1		
104.3	S2	
105.0		
107.5	108.6	
108.3	MG3	
109.5		
109.85		
110.55	SM3	
111.5		
112.05		

Lithological Description

- 102.1 - 103.0 : Grès fin, gris-vert, massif dur
- 103.0 - 104.3 : Grès fin, gris-vert, massif, tendre.
- 104.3 - 105.0 : Marne bigarrée, grumeleuse, parfois plaquetée, tendre à très tendre, localement broyée, sensible.
- 105.0 - 107.4 : Marne kaki et rougeâtre, plaquetée, assez dure, avec zones ± grumeleuses et tectonisées vers 105.5 m, et 106.0 m. De 106.55 à 107.4 m zone un peu grumeleuse avec fracture subverticale fermée, irrégulière.
- 107.4 - 108.3 : Marne gréseuse violacée puis gris-vert, massive, assez dure dans l'ensemble.
- 108.3 - 109.5 : Marne bariolée, avec petites taches rouges vers 109.15 m, plaquetée, feuilletée et grumeleuse de 108.95 à 109.1 m, tendre, sensible.
- 109.5 - 109.85 : Marne bariolée, grumeleuse, parfois altérée, très tendre, sensible.
- 109.85 - 110.5 : Marne finement gréseuse, grise et kaki, plaquetée à massive, assez dure, avec fracture verticale de 109.9 à 110.5 (effet du forage ?)
- 110.5 - 111.5: Marne gréseuse gris-vert, massive à plaquetée, dure à très



GIBB



SEI INGENIERIE

CERN - LHC PROJECT- POINT 5

COMPOSITION OF A TYPICAL
MG GEOTECHNICAL ZONE

J96107A

Date
MAY
1996

Figure
7.6

Extract from Borehole SLHC 33 log

Depth Geotechnical Legend
(m BGL) Unit

99.1	
99.85	
100.25	100.2
101.2	SM4
101.65	
102.2	
103.1	SS1
103.7	
104.7	104.5
	SW1
	105.1
106.0	105.7
	MG3

Lithological Description

- 99.1 - 99.85 : Grès fin verdâtre, avec galets mous, tendre, avec niveaux marno-calcaires au sommet et à la base.
- 99.85 - 100.25 : Mame noirâtre puis kaki, plaquetée, de dureté moyenne, sensible.
- 100.25 - 101.2 : Mame gréseuse grise, massive à plaquetée, dure à très dure avec petit épisode marneux de 100.75 à 100.85 m.
- 101.2 - 101.65 : Mame feuilletée et grumeleuse, bigarrée, tendre, sensible avec fractures obliques.
- 101.65 - 102.2 : Grès marneux, très fin, gris-vert, très dur.
- 102.2 - 103.7 : Mame gréseuse, gris-vert, massive, dure à très dure, peu altérable, avec zone plus marneuse, moins dure, plus sensible et faiblement tectonisée de 103.1 à 103.55 m.
- 103.7 - 104.7 : Grès fin gris-vert, un peu marneux, massif, en majorité très dur.
- 104.7 - 106.0 : Grès fin, gris-vert, massif, tendre.
- 106.0 - 107.5 : Mame grumeleuse bigarrée, tendre, sensible, abîmée au forage.



CERN - LHC PROJECT - POINT 5
COMPOSITION OF TYPICAL
SS AND SW GEOTECHNICAL ZONES

J96107A

Date
MAY
1996

Figure
7.7

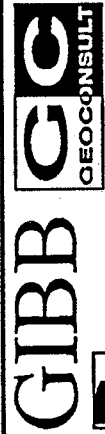
Extract from Borehole SLHC 36 log

Depth (m BGL) Geotechnical Unit Legend

90.3	MG5	
90.8		
93.4	SM5	
94.0		
96.0	SS2	
97.3		
98.35	91.8	
98.35		
99.3		

Lithological Description

- 90.3 - 90.8 : Marnes grises et violacées, grumeleuses, tectonisées, tendres à très tendres, sensibles.
- 90.8 - 91.45 : Marnes grises et kaki, plaquetées, dures.
- 91.45 - 92.4 : Marnes bariolées, très faiblement grumeleuses, assez dures.
- 92.4 - 93.4 : Marnes grises et kaki, violacées à la base, plaquetées à feuilletées, assez dures.
- 93.4 - 93.7 : Marnes rougeâtres, assez grumeleuses, avec fractures subverticales ± discontinues vers 93.5 à 93.7, tendres.
- 93.7 - 94.0 : Marnes rougeâtres puis grises, feuilletées à plaquetées, dures.
- 94.0 - 96.0 : Marnes gréseuses gris-vert panachées de kaki par endroits, massives à plaquetées, plus marneuses vers 95.2, avec niveau de grès fin de 95.4 à 95.6 m, très dures, peu altérables.
- 96.0 - 96.7 : Marnes kaki, localement violacées, plaquetées à feuilletées, moyennement dures, un peu grumeleuses et tendres vers 96.6 m, altérables.
- 96.7 - 97.2 : Marnes finement gréseuses, grises à taches vertes, massives, dures.
- 97.2 - 97.3 : Marnes bigarrées, feuilletées et grumeleuses, légèrement altérées; très tendres, sensibles.
- 97.3 - 98.0 : Grès très fins, ± marneux, gris-vert, massifs, très durs.
- 98.0 - 99.3 : Marnes gréseuses, à grès fins marneux à la base, gris-vert, plaquetées, dures à très dures, avec zone plus marneuse feuilletée de 98.35 à 98.5 m.



SEI INGENIERIE

CERN - LHC PROJECT- POINT 5

COMPOSITION OF A TYPICAL SM GEOTECHNICAL ZONE

J96107A

Date

MAY 1996

Figure

7.8

8. HYDROGEOLOGY

8.1 Introduction

The geological succession in the vicinity of Point 5 is discussed in detail in Section 6. The superficial glacial deposits are known to be water bearing and indeed are exploited to the north of the Point Five site for potable supply. The volume, direction and velocity of flow and the thickness of these water bearing units are crucial factors in the design and construction of the proposed shafts and caverns.

8.2 Water Bearing Units

Within the glacial moraines, both the sandy gravels (Unit 6a of the regional lithostratigraphic classification) and the thick cobbly moraine (9a) are considered to be aquifers within the area (GADZ 1996), and are henceforth referred to as the upper and lower aquifers respectively. Underlying the upper aquifer, the silty-clay and silty moraines and the silty gravel (Units 7di, 7ci and 7ac) are aquitards separating the lower and upper aquifers. Underlying these superficial deposits, the molasse bedrock is not exploited as an aquifer but is known to contain potentially water-bearing sandstone units associated with moisture-sensitive silty clays.

In the south of the site (Boreholes SLHC 34, 35, 36, 38, 39), the upper aquifer (6ac and a) is on average, approximately 10 m thick and is separated from the lower aquifer by a thick layer (maximum 21 m, minimum 19 m) of the silty-clay units (7d, 7c and 7ac).

In contrast, in the north of the site (Boreholes LHC 30, 31, 32, 33, 37), the upper aquifer thickens to an average 22 m at the expense of the silty-clay units. As a result the two aquifers are separated by a thinner layer (maximum 10 m, minimum 5 m) of silty gravel (7ac). This thickening of the upper aquifer to the north may represent a channel feature incised within the underlying silts and clays, although evidence for this is slight and some uncertainty remains.

The lower aquifer (9a) varies in thickness over the site from a minimum of 12 m to a maximum of 21 m.

8.3 Hydrogeological Testing

During the main LHC site investigation, several types of hydrogeological test were carried out during the period October 1995 to February 1996 and are discussed in turn below.

8.3.1 Pump Tests

A total of six pump tests were carried out within the upper and lower aquifers, the results of which are summarised in Table 8.1. Pump tests were not carried out within the molasse. Each test comprised five increasing steps of constant drawdown. As a validation exercise, the data provided was analysed using the method of Hvorslev (BS5930:1981, Section 21.4.6a) and derived values of hydraulic conductivity were consistent with those presented in the Factual Report.

In two boreholes, flow rates were insufficient to proceed with a pump test. The rate of recovery of the test zone was therefore monitored (in effect a rising head test). Using the method of Horslev (BS5930:1981 Section 21.4.6b) hydraulic conductivity values consistent with those presented in the Factual Report have been derived. Values summarised in Table 8.1 are therefore as presented in the Factual Report.

Table 8.1 - Summary of Pump Tests

Borehole No.	Test Type	Test Interval (maSL)	Geological Unit	Hydraulic Conductivity (m/s)
SLHC 30	Step	494.2 - 493.0	6a : upper aquifer	4×10^{-4}
	Step	466.7 - 463.7	9a : lower aquifer	3×10^{-3} (uncertain)
SLHC 31	Step	495.3 - 494.25	6a	8×10^{-4}
	Step	465.35 - 462.75	9a	5×10^{-4}
SLHC 33	Step	489.2 - 487.2	6a	1.5×10^{-3}
	Step	475.3 - 472.8 (471.5)	9a	9×10^{-5}
SLHC 34	Rising	473.9 - 471.4	9a	5×10^{-5}
SLHC 35	Rising	476.75 - 475.55	9a	3 to 5×10^{-5}
SLHC 36	Step	476.15 - 473.85	9a	1 to 2×10^{-4}
SLHC 37	Step	12.85 - 15.0	6a	2×10^{-3}

No flow/low permeability between 472.8 and 471.5 maSL

From the pump tests, average values of hydraulic conductivity of 1×10^{-3} m/s for the upper aquifer and 2×10^{-4} m/s for the lower aquifer can be derived. These values are consistent with those generally reported for silty and sandy gravels (Freeze and Cherry, 1979).

8.3.2 Borehole Packer (Lugeon) Tests

A total of 18 packer tests was carried out within the unweathered molasse bedrock, covering the proposed elevation of the shaft and cavern construction. Results of these tests are summarised in Table 8.2. No tests were carried out within the moraine deposits. These tests were carried out to investigate the hydraulic characteristics of any open discontinuities, principally in the upper part of the molasse. Where possible, the test comprised seven stages at pressures between 2.5 and 10 bars. In 16 of the 18 tests undertaken, no flow was measured during the first four stages of increasing pressure and the tests were thus terminated at this stage. The sensitivity of the flowmeters used is not quoted, but assuming this to be 0.4 l/min (the lowest flow rate known to be measured from the Factual Report) and using the maximum pressure of 10 bars, a minimum hydraulic conductivity of 9×10^{-9} m/s can be derived from these tests.

The low permeability of the Molasse at this site has been confirmed by the lack of any observed moisture or seepage in the LEP tunnel at Point 5.

Table 8.2 - Summary of Packer Tests

Borehole No.	Test Interval (maSL)	Hydraulic Conductivity (m/s)
SLHC 30	455.3 - 450.3	9×10^{-8}
	446.5 - 441.5	$< 9 \times 10^{-9}$
	437.4 - 432.4	$< 9 \times 10^{-9}$
	432.4 - 423	$< 9 \times 10^{-9}$
SLHC 32	456.5 - 453	$< 9 \times 10^{-9}$
	452.5 - 441.25	$< 9 \times 10^{-9}$
	425.5 - 410.5	$< 9 \times 10^{-9}$
	431.9 - 422.5	$< 9 \times 10^{-9}$
SLHC 33	409.3 - 403.3	$< 1 \times 10^{-8}$
SLHC 34	455.6 - 450.1	$< 9 \times 10^{-9}$
	449.3 - 440.1	$< 9 \times 10^{-9}$
	439.2 - 425.4	$< 9 \times 10^{-9}$
	424.4 - 414.4	$< 9 \times 10^{-9}$
SLHC 35	460.55 - 453.65	$< 9 \times 10^{-9}$
SLHC 36	456.35 - 448.35	$< 9 \times 10^{-9}$
	448.35 - 442.35	$< 9 \times 10^{-9}$
	442.35 - 431.75	$< 9 \times 10^{-9}$
	432.35 - 422.85	$< 9 \times 10^{-9}$

In some boreholes, the packer tests were carried out over several successive intervals, covering all lithologies encountered within the molasse, including sandstone units. A maximum hydraulic conductivity of 9×10^{-8} m/s was obtained at a level above that of the proposed cavern in Borehole LHC 30. All other tests indicated the hydraulic conductivity of the molasse to be less than 1×10^{-8} m/s.

No other hydrogeological information is available for the molasse.

8.3.4 Piezometer Installations

After completion of drilling, dual 2½" and/or 3" diameter piezometers were installed in each borehole, nested in order to monitor the upper and lower aquifers respectively, and separated by a clay and cement plug through the intervening silty-clay units. Installation details are given in the Factual Report (GADZ 1996a). No piezometers were installed within the molasse bedrock. Water levels were monitored every 3 - 4 days during January and February 1996. Average and maximum water levels for each piezometer during this period are reproduced in Table 8.3.

Table 8.3 - Summary of Piezometer Readings

Borehole No.	Upper Aquifer MAX. Water level (maSL)	Upper Aquifer AVG. Water level (maSL)	Lower Aquifer MAX. Water Level (maSL)	Lower Aquifer AVG. Water Level (maSL)
SLHC 30	502.56	500.39	501.18	499.04
SLHC 31	502.57	500.38	500.84	498.80
SLHC 32	502.27	500.88	500.97	499.45
SLHC 33	502.46	500.27	500.81	498.90
SLHC 34	502.12	500.16	500.70	498.64
SLHC 35	502.28	500.34	500.71	498.95
SLHC 36	502.38	499.98	500.88	498.88
SLHC 37	503.15	500.91	501.14	499.15
SLHC 38	501.89	499.80	500.82	498.90
SLHC 39	500.68	500.58	499.16	499.12

Piezometric levels for the upper aquifer are 7 to 9 mbGL and 9 to 10 mbGL for the lower aquifer. It is notable from Table 8.3 that the piezometric surface or hydraulic gradient is virtually level for both the upper and lower aquifer, average water levels varying only a maximum of 1.1 and 0.8 metres respectively.

The distribution of piezometric levels indicates groundwater flow towards the south-east in both the upper and lower aquifers, although this statement should be tempered with the knowledge that variations in level are within the bounds of measurement error. Consistency in the direction of flow indicates a degree of hydraulic connection between the two aquifers.

From the piezometric levels for the upper aquifer, a hydraulic gradient of 0.004 m/m can be derived. From Section 3.1, the average hydraulic conductivity is 1×10^{-3} m/s. Assuming a porosity of 20%, an average linear velocity, v' , through the upper aquifer of 2×10^{-5} m/s (1.9 m/day) can be derived from Darcy's Law.

For the lower aquifer, knowing a hydraulic gradient of 0.004 m/m, an average hydraulic conductivity of 2×10^{-4} m/s and assuming a porosity of 20%, an average linear velocity, v' , of 4×10^{-6} m/s (1.4 m/day) can be derived. The maximum hydraulic head observed in the lower aquifer in Boreholes 30 and 32 is approximately 42 metres above the base of the aquifer.

In all boreholes, the piezometric level of the upper aquifer is an average of 1.5 metres higher than that of the lower aquifer. This indicates the presence of a semi-confining layer between the two aquifers, in turn suggesting the silty-clay units (7d, 7c, 7ac) to be of low permeability. As a result of the head difference, a downward flow potential exists from the upper to the lower aquifer through this semi-confining layer.

In the northern part of the site, covering the proposed location of the shaft and cavern, the minimum thickness of the semi-confining layer is 5 metres of silty gravels. Assuming a hydraulic conductivity of 1×10^{-7} m/s and a porosity of 15%, an average linear velocity, v' , of water downwards through this layer, of 1×10^{-7} m/s (0.01 m/day), can be derived using Darcy's Law.

In the southern part of the site, the semi-confining layer is a minimum 19 metres of silty-clays and gravels. Assuming an average hydraulic conductivity of 5×10^{-8} m/s and a porosity of 15%, a downward velocity of 2×10^{-8} m/s (0.002 m/day) can be derived. From the extent of the data, in terms of observational data, it appears that the two aquifers can be considered separately in subsequent design work, although potential leakage paths are provided by Borehole LHC30 and ground freezing boreholes used for the earlier shaft PX54 construction.

8.3.5 Flowmeters

A downhole flowmeter was used within several boreholes in order to assess the origin of flow and flow rates. However, changes in flow are sensitive to changes in borehole diameter, such as occur as a result of washouts and collapses, and hence the data must be interpreted with care. In some boreholes, the earlier installation of piezometers prevented the use of the flowmeters without additional injection of water into the system. With the system at rest, flowmeter measurements did not show any significant natural circulation within Boreholes 30 and 39.

Flowmeters were only used within the moraine deposits. Constant inflows were indicated through both aquifers with little or no flow through the intervening silty-clays, indicating homogeneous porous media conditions in the aquifers and low permeability within the silty-clays. This tends to confirm that the silty clays form a semi-confining layer between the two aquifers.

8.3.6 Tracer Testing

Two phases of tracer testing were carried out between November 1995 and February 1996 in order to evaluate the direction and speed of water flow within the aquifers. In each phase, several discrete injections into individual boreholes (7 - 15 minutes duration) of differing tracer compounds were executed, whilst pumping at appropriate depths in downstream boreholes. These phases are summarised in Table 8.4 below. The tests are described in detail in GADZ 1996a.

Table 8.4 - Summary of Tracer Testing

FIRST PHASE TESTING (9 injections 28/11 - 1/12/95)			
Upper Aquifer		Lower Aquifer	
Injection	Pumping	Injection	Pumping
BH 30 Eosine		BH 30 Sulfo-rhodamine G	
BH 31 Naphtionate	BH 33	BH 31 Uranine	BH 34
BH 32 KI	18 mbGL	BH 32 LiCl	31 mbGL
BH 35 NaCl		BH 33 SrCl ₂	
		BH 35 KNO ₃	
SECOND PHASE TESTING (6 injections 24/2/96)			
Upper Aquifer		Lower Aquifer	
Injection	Pumping	Injection	Pumping
BH 30 Sulfo-rhodamine G	BH 39	BH 30 Eosine	BH 39
BH 31 Uranine	10.5 mbGL	BH 31 Naphtionate	37 mbGL
BH 32 LiCl		BH 32 KI	

This testing indicated that the two aquifers were not completely independent, with some flow occurring from the upper to lower aquifer. This direction of flow is consistent with the head differences observed in the piezometer installations and discussed in Section 3.3. The weak concentrations of tracer recorded at the downstream boreholes indicates significant lateral circulation within the lower aquifer.

GADZ 1996a gives the following effective velocities, based on peak arrivals at the receiver boreholes, for groundwater flow within the upper and lower aquifers:

Upper Aquifer	First Phase $V_e = 0.03$ m/h	Second Phase $V_e = 0.13$ m/h
Lower Aquifer	First Phase $V_e = 0.06 - 0.13$ m/h	Second Phase $V_e = 0.13 - 0.3$ m/h

It is stated that these values are an underestimate of the effective velocity due to the overestimate of the flow thickness. Velocities are therefore expected to be about 0.13 m/h (3.12 m/day) for the upper aquifer, and up to about 0.3 m/h (7.2 m/day) for the lower aquifer. These values are the same order of magnitude as those calculated in Section 3.3.

8.4 Hydraulic Behaviour

- * The superficial deposits contain two major aquifers:

Upper : Unit 6a (& 6ac), Sandy Gravels

Average hydraulic conductivity 1×10^{-3} m/s, 10 - 22 metres thick

Lower : Unit 9a, Thick Cobbly Moraine

Average hydraulic conductivity 2×10^{-4} m/s, 12 - 21 metres thick

- * The aquifers are separated by a semi-confining layer of silty-clay moraine. Some localised hydraulic connection occurs through this layer.
- * Piezometric levels indicate very low hydraulic gradients and a south-easterly flow direction for both aquifers.
- * Hydraulic head in the upper aquifer is an average of 1.5 m above that of the lower aquifer, therefore a potential for downward flow exists. Estimated downward flow velocity using assumed hydraulic conductivity is 1×10^{-7} m/s (0.01 m/day).

- * The upper aquifer is thinner to the south and the semi-confining layer has a maximum thickness of 19 -21 m of silt, clays and silty gravels. In the north, the upper aquifer unit thickens at the expense of the lower permeability silts and clays, reducing them to a minimum thickness of 5 m of silty gravels only.

- * From piezometric levels, average linear flow velocity in the upper aquifer has been estimated as 2×10^{-5} m/s (1.9 m/day). Average linear flow velocity in the lower aquifer is estimated as 4×10^{-6} m/s (1.4 m/day). Flow velocities calculated from tracer testing are about 3.6×10^{-5} m/s (3.12 m/day) in the upper aquifer and up to about 8.3×10^{-5} m/s (7.2 m/day) in the lower aquifer.

- * The molasse has low permeability (94% of tests $<1 \times 10^{-8}$ m/s), though with a local maximum in a single test of 9×10^{-8} m/s. Therefore, there are no indications of a hydraulically-connected fracture network within the molasse.

9. GEOTECHNICAL CHARACTERISATION

9.1 Moraine

9.1.1 Introduction

During the main LHC investigation ten boreholes were sunk through the moraine around the site. No laboratory testing was carried out on samples from the moraine and considerable reliance has to be made on the description in the borehole logs and the in situ testing results, as presented in the Factual Report (GADZ 1996a). The following information has been used to assess the description and engineering parameters for the moraine:

- (a) borehole log descriptions
- (b) soil classification to the Swiss Standard SNV 670 008
- (c) standard penetration test results
- (d) pocket penetrometer results

It is assumed that the pocket penetrometer results record the unconfined compressive strength (UCS). Therefore, the undrained shear strength of the cohesive bands within the moraine is given by dividing the UCS value by two.

9.1.2 Lithological Descriptions

As described in Section 6, the regional lithostratigraphic classification for materials within the moraine was applied during logging, and the various materials were correlated across the site (Figures 6.1 to 6.3). The lithostratigraphic nomenclature has been used in previous investigations, and the Synthesis Report (GADZ 1993) provides a limited number of data for units 7cd and 9ac, which can be used as reference data. However, the high general variability of the moraine deposits have to be considered.

9.1.3 Geotechnical Parameters

Modulus of Elasticity

In the absence of site specific laboratory test data, the modulus of elasticity can be estimated from the Standard Penetration Test N value, as follows:-

For granular materials, recourse has been made to CIRIA Report 143 (1995), to enable an estimate of the vertical modulus of elasticity, E'_v , to be made. Since this deposit has been subjected to at least 400m of glacial loading, the deposit is overconsolidated. On this basis a conservative, initial estimate of E'_v at strains consistent with normal foundation loading and factors of safety is given by:-

$$E'_v = 1.5 N \text{ (MPa)} \quad \text{where } N \text{ is the SPT blow count.}$$

For cohesive materials, reference is made to CIRIA Report 143 (1995), which indicates that for low plasticity clays, the value of E'_v can initially be taken conservatively as:-

$$E'_v = 1.0 N \text{ (MPa)}$$

The horizontal modulus of elasticity is likely to be greater than the vertical modulus by a factor of 1.5. However, for the present it would be prudent to adopt a value equal to the vertical modulus. The SPT blow counts were generally found to vary from values in excess of 50 near surface, to values in excess of 100 below about 25m depth. Some boreholes indicated zones of lower blow count values but these were probably indicative of clay bands.

Drained Angle of Friction

For granular materials, the drained angle of friction can also be estimated from the SPT blow count. The relationship between drained angle of friction, ϕ' , and SPT blow count has been proposed in CIRIA Report 143 after work by Peck, Hanson and Thornburn (1974), and is a function of vertical effective stress. From the distribution of SPT data, a maximum of 40° value of ϕ' is recommended for designs.

For cohesive materials, the drained angle of friction can be estimated from the Plasticity Index (PI) using the relationship proposed by Kenney (1959). Whilst there are no site specific PI results available for the moraine, the clayey component is described as low plasticity in the SNV classification shown on the borehole logs. Assuming a PI of less than 20%, the corresponding value of ϕ' would be 30° .

Using the methods outlined above, together with a knowledge of the geotechnical properties of fluvio-glacial materials within the Geneva Basin in the Geneva area, the following ranges of geotechnical parameters were identified (Table 9.1).

Table 9.1 - Typical Ranges of Geotechnical Parameters for Moraine Units

Unit	γ (kN/m ³)	ϕ' (deg)	c' (KPa)	E (MPa)
6a Gravel	23.0 - 23.5	35 - 37	0	50 - 80
6ac Silty gravel	23.0 - 23.5	33 - 35	0 - 5	40 - 60
6d2 -6c2 Silty clayey sand Sandy clayey silt	20.0	28 - 30	6 - 3	7 - 9
7d1 Silty clay	23.0 - 23.5	30 - 31	15 - 20	60 - 80
7c1 Sandy silt	23.5 - 24.0	32 - 34	20 - 25	80 - 120
7ac Silty gravel	23.5 - 24.0	32 - 35	15 - 20	100 - 150
9a Sandy gravel	23.5	40 - 42	Generally >15	>200

9.1.4 In-situ Horizontal Effective Stresses

No measurements of in-situ horizontal stress were made within the moraine during the site investigation. However, a preliminary estimate can be made from an assessment of the stress history. It is believed that the Würmian moraine strata were subjected to unloading from an ice sheet, up to 400m thick. In order to estimate the in-situ horizontal stress regime, the following assumptions are made:-

- (i) the moraine is deposited by sedimentation, with the initial horizontal effective stresses approximately 0.5 times the initial vertical effective stresses
- (ii) the depth of erosion is unknown and has been ignored

(iii) the soil responds to ice unloading as an elastic, isotropic medium under conditions of zero lateral strain

(iv) the Poisson's Ratio is given by $\nu'=0.25$

From the above assumptions, it can be shown that the reduction in horizontal effective stress, $\Delta\sigma'_h$, due to ice unloading, is given by:-

$$\Delta\sigma'_h = (\nu'/(1-\nu')) \Delta\sigma'_v$$

where $\Delta\sigma'_v$ is the reduction in vertical effective stress due to ice unloading. The current value of Coefficient of Earth Pressure At Rest, K_o , is given by:

$$K_o = \sigma'_h / \sigma'_v$$

where σ'_h is the in-situ horizontal effective stress, and σ'_v is the vertical effective stress.

The present in-situ value of K_o can be estimated from the in-situ value of σ'_h , calculated from the value during deposition and modified by the change occurring due to unloading.

Table 9.2 below gives calculated values of σ'_h , σ'_v , and K_o :-

Table 9.2 - Estimates of in situ stress magnitude within the Wurmien moraine (Units 7-9)

Depth below ground level (m)	σ'_h (kPa)	σ'_v (kPa)	K_o
*10	717	180	4.0
*20	767	280	2.7
30	817	380	2.1
40	867	480	1.8
50	917	580	1.6

* The upper 10 to 20 metres of the moraine are typically fluvio-glacial deposits (unit 6). These are generally normally consolidated, without overconsolidation due to ice loadings. K_o values will typically be in the range 0.4 to 0.55 for this material.

9.1.5 Foundations for Surface Structures

Generally, the near surface geology should be suitable for shallow foundations for lightly to moderately loaded structures. For example, the settlement of a 2m by 2m pad foundation operating at a net allowable bearing pressure of 300 kPa on to the very dense gravels, will be in the order of 10mm to 15mm. The presence of a very dense gravel layer, some 2.5m to 3m thick, overlying any clay bands should ensure that these bands will not be overstressed.

In the vicinity of Borehole SLHC 37, firm to stiff clay exists over the top 5m and shallow foundations at reduced bearing pressures would be more appropriate. For instance, the settlement of a 2m by 2m pad foundation, operating at a net allowable bearing pressure of 175 kPa, is likely to be in the order of 25mm.

Raft foundations are a possible option, particularly on the very dense gravels. The viability of this type of foundation will depend upon the total and differential settlement criteria for the structures.

Heavily loaded structures may need to be founded on a piled foundation. It is likely that a bored pile solution would be appropriate, since driven piling would be difficult in these ground conditions where high SPT values were encountered.

9.2 Molasse - Time Independent Assessment

9.2.1 Key aspects of Rock Mass Behaviour

The engineering behaviour of the molasse formation will be closely related to the intrinsic nature of the rock mass (stratified, bedded and moisture sensitive) and to the nature and extent of construction-induced overstress and disturbance. The responses are in general complex and may vary from crown/haunch overbreak and invert heaving to peripheral overstress, also involving progressive time-dependant effects. Shear overstressing along bedding planes (both incipient and pre-existing) is a well-understood stability mechanism in the generation of such effects.

The following are considered to be key aspects of the engineering behaviour of the molasse:

- a) The non-homogeneity and variability of rock materials,
- b) the rock mass comprises a well-defined stratigraphic and layered system of alternating rock material properties.
- c) the overall weak nature of the rock components. For example, up to 60% of the rock materials types have a uniaxial compressive strength (UCS) in the range 5 to 8 MPa. With the likely depth of the caverns (75 to 100 m overburden) and inferred high horizontal stresses, mild overstressing is considered to be likely for some of the weak elements of the rock mass.
- d) Time, moisture and deformation dependant behaviour.

The weak, marly rock types are known to exhibit complex behaviour, particularly in association with moisture changes and relatively high stresses. For a preliminary evaluation it suffices to focus on the basics of elastic - plastic response for the intact materials coupled with stress and displacement-dependant shear behaviour of the inferred structure. The model behaviour is based on the available data base of measured parameters, core observations and expert judgement.

It is proposed that rock material strength is represented by an elastic-plastic failure criteria, such as the Mohr-Coulomb criterion. It is considered that the database used to derive rock material strength parameters is too limited to allow reliable application of a realistic, more complex (i.e. non-linear) failure criteria with sufficient confidence. Parameters will be determined for each of the four geotechnical unit types identified.

Discontinuities within the rock mass predominantly comprise bedding partings of very low or zero tensile strength, between alternate units, and may be characterised as pre-existing bedding planes. In addition, to reflect the pervasive bedded nature of the rock mass, incipient bedding discontinuities may also be characterised for SM, SS and SW units, for inclusion in numerical simulations. Thin MG units, previously discussed, may be represented as weak, compliant interfaces, and parameters are derived accordingly.

9.2.2 Basic Rock Material Properties

A summary of data acquired during the investigation for the LEP project is presented in Table 9.3 (GADZ 1993). A different material classification was used in the GADZ report, but the subdivisions are considered to broadly agree with those defined in this report (Section 7.0). Figures 9.1 to 9.3 shows summary histograms for data acquired during the LHC investigation for all geotechnical units (defined in Section 7.0) for uniaxial compressive strength, tensile strength and deformation modulus. The data used to generate these histograms were taken from both the Point One and Point Five databases, in order to generate datasets of a reasonable size. There is no concern about material differences between these sites. The frequency distributions can be compared with the data presented in Table 9.3.

Table 9.3 - Summary of Basic Rock Material Parameters from the LEP investigation

Rock Material	W%	σ_c (MPa)	E_c (MPa)	σ_t (MPa)
Sandstone weak	7.6 (3.4 - 12)	10.6 (3.8 - 14.9)	1181 (214 - 2750)	0.8 (0.22 - 1.6)
strong	4.3 (1.7 - 6.5)	22.8 (15 - 34.8)	2984 (1000 - 6300)	2.2 (0.9 - 3.9)
very strong	2.9 (1.2 - 5.2)	48.4 (35 - 100)	8763 (3830 - 22000)	3.5 (1.5 - 7.3)
Sandy marl	6.0 (3 - 8.7)	13.4 (4.6 - 24.6)	1484 (190 - 3630)	1.5 (0.6 - 3.0)
Marl	8.8 (4.2 - 12.3)	5.7 (0.9 - 15)	423 (225 - 1590)	0.9 (0.2 - 3)

It can be seen that the two datasets are generally consistent. In accordance with the geotechnical units described in Section 7.2, the following basic rock material parameters were selected for design purposes:

Table 9.4 - Selected Basic Rock Material Parameters

Geotechnical Unit	σ_0 (MPa)	σ_t (MPa)	E (MPa)	V	K (GPa)	G (GPa)
Marl grumeleuse (MG)	5	0.5	1000	0.35	1111	370
Marl (laminated) (ML)	10	1.0	2800	0.25	1867	1120
Transitional (sandy marl, marly sandstone,) (SM)	20	2.0	4000	0.25	2667	1600
Sandstone Weak (SW)	10	1	2000	0.25	1333	800
Strong (SS)	40	4	8000	0.25	5333	3200

It is generally accepted that the geotechnical properties of the marl material within the molasse are sensitive to changes in moisture content. This is illustrated in Figure 9.4 which shows a graph of moisture content against uniaxial compressive strength, together with a frequency distribution for natural moisture content determination, for marl grumeleuse. The resultant trend shows a correlation between increasing UCS and decreasing moisture content, as would be expected. The modal moisture content (assumed to be the in situ value) for this material is some 8-9% as shown on the moisture content histogram, corresponding to a UCS value of approximately 4 - 5 MPa. This can be compared with the histogram for marl grumeleuse UCS (Figure 9.1), which indicates a modal value of some 8 MPa, which would therefore appear to be erroneously high. Such effects have been taken into account in the selection of conservative, basic material parameters.

9.2.3 Rock Material Strength

The triaxial strength of the various rock materials was assessed by analysis of the triaxial test results. Initially, tests were grouped together according to the material description given in the test data sheet, before finally being analysed in terms of the established geotechnical donation.

The peak c, ϕ_p parameters were determined by linear regression of the test data using the ROCKDATA program. Residual ϕ_r ($c=0$) values were calculated from the results from each multistage test. The procedure involved determination of the shear and normal stress (σ, τ) pairs from each stage and from all tests on the same material and then processing by linear regression of all σ, τ pairs to derive the best fitted line ϕ_r value. The derived parameters are summarised in Table 9.5 below. It should be noted that the datasets are limited in size, and selection of design parameters will take account of this.

Occasional ϕ_{res} values higher than ϕ_{peak} values were presumably due to the limited number of tests available per group and the bias that limited test data may have on linear regression derived, c, ϕ values. This apparent ambiguity may be explained by the so-called 'residual' friction angle in the triaxial test corresponding to an induced fracture and the measured frictional resistance being influenced by the surface roughness of the induced fracture. Such differences however, cannot be regarded to be of significance at field scales.

Table 9.5 - Peak and residual shear strength parameters from triaxial tests

Rock Type (according to sample description)	Peak Parameters		Residual (c=0)	No of tests
	c (MPa)	ϕ_p (°)	ϕ_r (°)	
Marl ("intact")	3.40	29.2	30.2	5
Weak marl	2.20	25.4	31.0	5
Thinly bedded Marl	1.25	38.0	36.8	9
Laminated Marl	2.05	29.4	33.4	3
Marl (Grumeleuse)				
Upper	1.5	24.8		
Lower	0.4	19.6	22 ± 5	6
Sandy marl	2.2	43.7	38.7	26
Marly sandstone	6.9	33.8	41.3	3
Sandstone strong	5.0	45	41.8	peak parameters assessed

It is of interest that the residual friction angle of the marl grumeleuse from the direct shear tests ($21 \pm 4^\circ$) is very close to the peak friction angles from the triaxial tests (19.6 to 24.6°), implying an ultimate strength state of the grumeleuse marls is very close, or at the residual state, due to the effects of past overstressing and associated shear straining.

Reanalyses of all data according to the geotechnical classification for the site yielded the following strength parameters given in Table 9.6. Intact marl has been retained as a reference case, for comparison with data given in the literature.

Table 9.6 - Strength parameters of the geotechnical units

Geotechnical Unit	Peak parameters		Residual (c=0)
	c (MPa)	ϕ_p (°)	ϕ_{res} (°)
Intact Marl (reference case)	3.40	29.2	30.2
Marl Grumeleuse (MG)			
Upper Bound	1.5	24.6	
Lower Bound	0.4	19.6	22 ± 5
Marl (laminated) (ML)	1.3	35	30.6
Sandy marl/Marly sandstone (SM)	2.2	43.7	38.7
Sandstone (strong) (SS)	5.0	45	41.8

A series of graphs with all data and the Mohr-Coulomb regressions is attached for reference of the data analyses (Figures 9.5 to 9.10).

9.2.4 Discontinuity Parameters

Discontinuity parameters were determined by analysis of direct shear test data. Direct shear tests were conducted parallel to both pre-existing discontinuities and incipient bedding (intact) in marl. The tests were conducted in reverse and forward cycles under different normal stresses. All results reported in the Factual Report were reanalysed and summarised in Tables 9.7 and 9.8.

Table 9.7 - Shear strength parameters for existing (open) bedding joints in Marl

Parameters	Linear M-C regressions c , ϕ_p	ϕ (Assuming $c=0$ & averaging all tests)	No. of tests
Peak	$c = 0.04$ Mpa	Average 36° Min 13° Max 74.6° Std dev 17.9°	17
Residual: Overall average		Mean 20.6° Min 13.0° Max 27.7° Std dev 4.3°	
Lowest bound		Mean 17.9° Min 10.5° Max 27.0° Std dev 4.5°	

Table 9.8 - Shear strength parameters for Incipient bedding joints (intact) in Marl

Parameters	Linear M-C regressions c , ϕ_p	ϕ (Assuming $c=0$ & averaging all tests)	No. of tests
Peak	Widely dispersed data Best fitted lines (assessed) provide: $c = 0.1 - 1.0$ Mpa $\phi = 30^\circ$		20
Residual Overall average		Mean 27.9° Min 10.8° Max 37.8° Std dev 5.9°	
Lowest bound		Mean 24.9° Min 10.8° Max 35.6° Std dev 5.3°	

From back-analysis of direct shear tests, the following Barton-Bandis indices were derived for existing and incipient bedding in marl:

Open bedding joints (marl)	JRC _o	= 10
	JCS _o	= 10 MPa
	Ø _r	= 20°
Incipient bedding joints (marl)	JRC _o	= 20
	JCS _o	= 15 MPa
	Ø _r	= 30°

A slight reduction in JCS_o was considered appropriate for the pre-existing bedding joints to allow for slight weathering effects (surface staining). The predicted envelopes in Figure 9.11 indicate the range of shear strength according to the above characterisation indices.

9.2.5 Summary of Selected Parameters for Molasse for Design

Tables 9.9 to 9.12 below present a summary of the selected design parameters for the geotechnical units and discontinuity types within the molasse.

Table 9.9 Rock Material Properties

Rock Materials	σ _c (MPa)	σ _t (MPa)	E (MPa)	ν (GPa)	K (GPa)	G (GPa)	C (MPa)	Ø (°)	
Marl grumeleuse (MG)	5	0.5	1000	0.35	1111	370	0.2	20	
Marl (laminated) ML	10	1.0	2800	0.25	1867	1120	1.0	35	
Transitional (sandy marl, marly sst.) (SM)	20	2.0	4000	0.25	2667	1600	1.0	40	
Sandstone	Weak (SW)	10	1	2000	0.25	1333	800	0.5	35
	Strong (SS)	40	4	8000	0.25	5333	3200	2.5	45

The following discontinuity parameters are expressed in terms of input parameters for the UDEC modelling code.

Table 9.10 Marl Grumeleuse Interface Properties

Parameter	Value
Joint Cohesion	0
Joint Friction Angle	20°
Joint Dilation Angle	0
Joint Normal Stiffness	2000 MPa/m
Joint Shear Stiffness	500 MPa/m
Joint Tensile Strength	0

Table 9.11 Existing (Open) Bedding Joints (Barton-Bandis Parameters)

Indices	Marl	Sandstone (weak)	Sandstone (strong)
JRC ₀	10	10	10
JCS ₀	10	10	40
∅ _r	20°	30°	30°
Aperture (mm)	0.2	0.2	0.2
Lo (m)	0.1	0.1	0.1
Ln (m)	0.5	0.5	0.5
Joint Normal Stiffness (MPa/m)	3e5	7e5	7e5
Joint Shear Stiffness (MPa/m)	400	650	650
Sigmac (Mpa)	15	10	40

Table 9.12 Incipient Bedding Joints (Mohr-Coulomb Parameters)

Parameters	Marl	Sandstone (weak)	Sandstone (strong)
Bulk Modulus (MPa)	2200	1333	5333
Shear Modulus (MPa)	1670	800	1333
Cohesion (MPa)	1.0	0.5	2.5
Friction Angle, ∅	40°	35°	45°
Joint Cohesion (MPa)	0.5	0.1	1.0
Joint Friction Angle, ∅	30°	35°	40°
Joint Tensile Strength	0.2	0.1	5

9.2.6 Parameter Uncertainty Assessment

In order to check the effect of critical parameters on overall behaviour, it is necessary to consider the influence of possibly lower bound parameters. Although the widespread application of sensitivity analyses is not advocated on this project, nevertheless, it is deemed prudent to check the effect of those parameters which could have a dominant influence.

In relation to the characterisation process, one key parameter is dominant, namely the shear strength characteristics of the bedding discontinuities in marl. Based on both actual strength measurements (see 9.2.4 above), and precedent data on marls, a lower bound shear strength corresponding to a ϕ value of 18° has been identified. This would apply to bedding discontinuities in marl as well as the marl grumeleuse interface conditions, and it would be prudent to investigate the effect of this value in the design process.

9.3 Molasse - Time Dependant Assessment

9.3.1 Swelling - Fundamental Considerations

The calcareous sediments (marls) within the Molasse at CERN, contain smectite, a clay mineral which is susceptible to swelling. The common mineral form of smectite is montmorillonite which occurs in various amounts within the marl and sandy marl constituents.

XRD analyses have been used to determine the clay content as outlined in the Factual Report (GADZ 1996). These analyses have indicated the clay percentages and proportions of smectite (montmorillonite) as indicated on the table in section 5.2.8 of the Factual Report (GADZ 1996).

9.3.1.1 Clay Mineralogy - Structure

Clay minerals are a group of hydrous sheet silicates. The 2:1 layer clays such as illite, vermiculite and the smectite group have a octahedral sheet linked to two tetrahedral sheets. There is extensive substitution of Mg and Fe for Al in the octahedral sheet and Al for Si in the tetrahedral sheet. The nature and the extend of this substitution determent the mineral type.

In the case of the common smectite - montmorillonite - Mg replaces some of the octahedral Al, for illite some of the Si is replaced by Al. Clay minerals are often present as interstratified or interlayered combinations of several clay mineral types; of particular concern are the interlayered illite/montmorillonites.

9.3.1.2 Swelling Phenomena

Swelling is caused by the interaction of polar molecules - typically water - with mineral surfaces. In montmorillonite the individual layers are weakly bound and under certain conditions each interlayer surface can hydrate leading to extensive swelling.

9.3.1.3 Crystalline Swelling

The adsorption of the layer of water on the surface of each montmorillonite layer occurs in a series of discrete steps; the resultant swelling has been termed 'crystalline swelling'. The adsorption results from a complex interaction between water molecules, mineral surfaces and the exchangeable cations. The basal spacing of montmorillonite increases stepwise from 0.98 nm to about 1.9 nm with increasing relative humidity corresponding to the addition of 3 to 4 layers of water.

The strains associated with crystalline swelling of montmorillonite can range up to about 95%. The associated pressures at zero strain are difficult to measure directly but have been estimated by various workers (Table 1). The pressures are very large, ranging from 2 MPa to 540 MPa depending on the exchangeable cation and the interparticle spacing. It can be seen that crystalline swelling pressures are of similar magnitude to stresses that lead to the failure of most rocks in uniaxial compression.

Table 9.13 - Estimates of the pressures associated with changes in interlayer spacings of montmorillonite in the range of crystalline swelling at 25°C (values are total stresses in MPa)

Spacing (mm)	Ca - Montmorillonite		Na - Montmorillonite	
	Van Olphen [7]	Bird [8]	Bird [8]	Spitzer [9]
1.25 - 1.00	540	150 - 250	150 - 250	88.0
1.55 - 1.25	250	50 - 60	50 - 60	-
2.00 - 1.85	120	25	25	7.1
2.00 - 1.85	-	-	-	2.4

It must be noted that pore smectites are not the only minerals prone to swelling; mixed layer minerals, of which one layer is smectite, will also swell. These include:

- Kaolinite - montmorillonite
- Montmorillonite - mica
- Illite - montmorillonite

9.3.2 Swelling Tests - Particular Observations

Swelling tests (Essais de Gonflement) using the Huder - Ambert procedure have been carried out on samples from both the Point One and Point Five boreholes. The individual test results are contained in Appendix 1 (Annexe R357) of the Synthesis Report (GADZ 1993).

The calcareous sedimentary rocks (marls) have been assessed in terms of their lithological descriptions based on the borehole logs which are further controlled and supported by other logging indications (calliper logs and sonic velocity sample tests).

The clay fraction of the marl beds in the molasse represents 30 to 55% of the mineral composition of the rock. The mixed layer minerals prone to swelling represent 15 to 40% of the clay fraction, or 8 to 15% of the rock.

Analysis of results from tests carried out according to the Huder-Amberg Method shows that the potential for swelling varies from less than 1% to 21%. All the samples tested parallel to the strata showed only minor swelling (less than 1.3%) except one sample which showed a potential for swelling of 10.8%. Swelling pressure in the majority of samples tested was less than 1780 kN/m^2 , except in two cases:

- Borehole SLHC 30, laminated marl at 93.2m depth, where the swelling pressure was estimated at 2500 kN/m^2 (maximum 3000 kN/m^2).
- Borehole SLHC30, multi-coloured marl at 110.7m depth where the swelling pressure equalled that of bearing load 1, 1780 kN/m^2 .

Unfortunately, it is not possible to produce a correlation between the clay mineral content and the swelling potential or swelling pressure, as the swelling tests and X-ray analysis were not performed on the same samples.

Two preliminary indices have been derived for initial evaluation of the results. These correspond to:

1. The swelling index (expressed as % strain change) for the unloading stress change in the range 100 kN/m^2 to 10 kN/m^2 . This is a short term test.
2. The swelling index (expressed as % strain change) for a 100 hour period for a low induced (vertical) stress of 15 kN/m^2 . This must also be considered as relatively short term.

These indices are considered relevant to the likely stress change and ultimate stress state of the rock mass particularly above the excavation crowns and below the inverts.

The summary indices are given in Table 9.14 and indicate the following:

1. The correlation between swelling behaviours and the marl type are indistinct and probably not amenable to further definition.
2. Swelling under nominal confinement (15 kN/m^2) is generally of the order of 5 - 7% for the 'purer' marls.
3. Weak laminated marls exhibit swelling of the order of up to 25% under nominal confinement .

4. Time dependant swelling is significant, particularly in the weaker marl units.

The data available are considered insufficient for detailed representative analysis but can be used to develop an initial indicative model.

9.3.3 Implied Behaviour

The implied behaviour that could potentially rise to significant swelling pressures and/or deformation will need to be considered in detail in relation to the excavation sequence and support methodology. Precedent data that are available both from CERN and other less critical rock types underline the potential significance.

An aspect of fundamental importance is the distribution of swelling pressures and in particular the development of localised concentrations of contact pressure on the support system and, possibly, lining of the cavern. The engineering effects and the potential implications on lining stresses need therefore to be addressed in this context.

In order to develop adequate confidence during detailed design, more specific data will be required which may include induced lining stress measurements and more detailed sample testing. Reassessment of the actual state will need to be validated via performance monitoring when the actual geotechnical conditions in the cavern have been exposed.

Table 9.14 - Summary of Swelling Test Data from the LHC Investigation

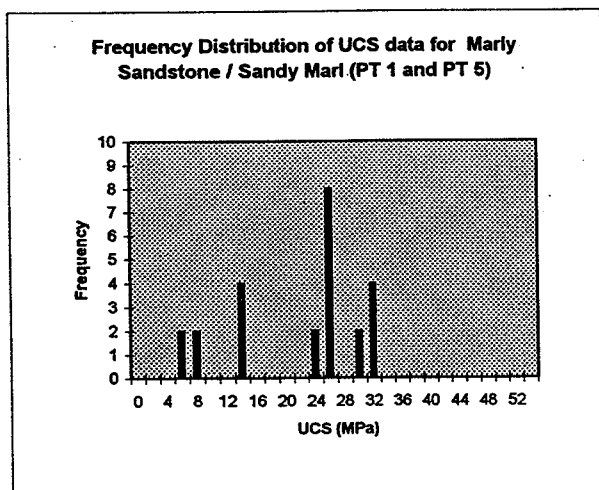
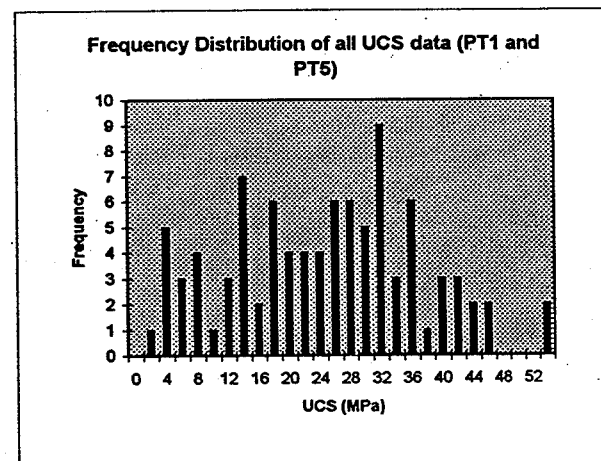
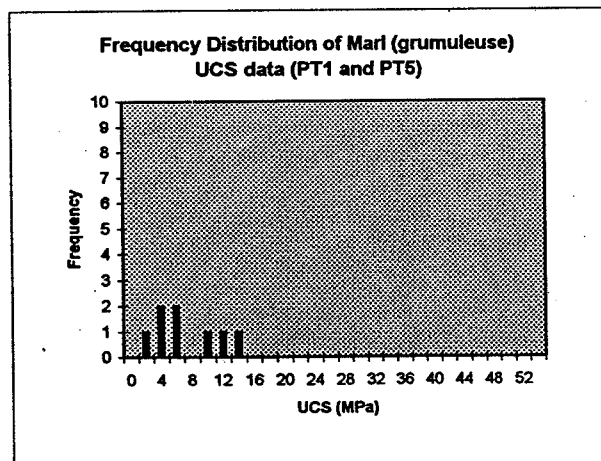
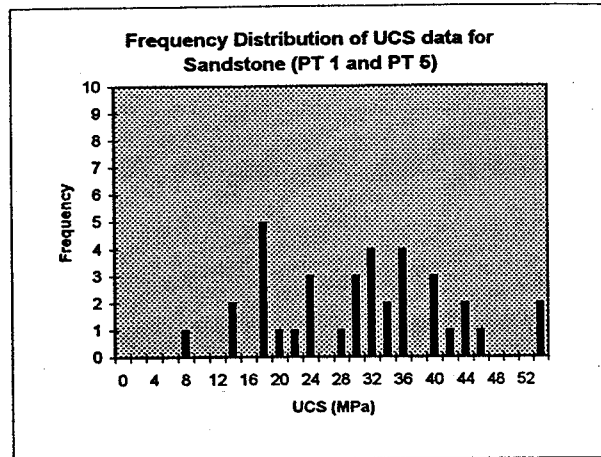
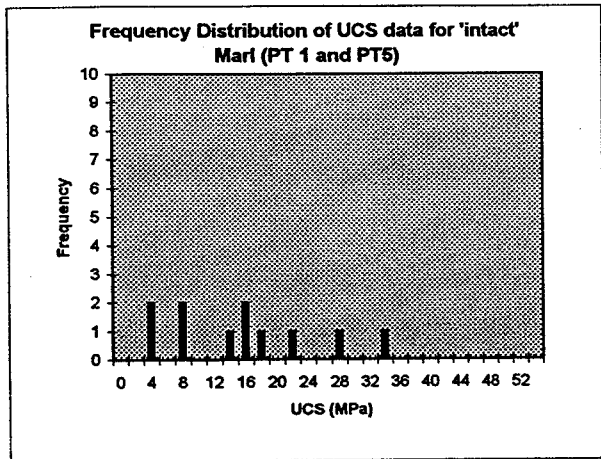
BOREHOLE	DEPTH	LITHOLOGICAL DESCRIPTION	LITHOLOGICAL TYPE	CERN SI %	100 HR SI %
POINT ONE					
20	77.20	Fine sandy marl, strong, laminated and locally grumeleuse	SM/MG	7.0	2++(1)
20	104.60	Slightly sandy marl, thinly bedded	SM	7.0	4++
20	87.05	Weak laminated marl	MG (=)	12	5+
22	81.10	Weak laminated marl	MG (=)	23	9+
22	92.80	Sandy marl, moderately strong to weak, grumeleuse	MG	3.5	1+
24	78.50	Marl, locally fine sandy, very strong, massive/grumeleuse	MG	1.4	0.3+
24	89.50	Marl, weak to very weak, laminated grumeleuse	MG	3.0	1+

BOREHOLE	DEPTH	LITHOLOGICAL DESCRIPTION	LITHOLOGICAL TYPE	CERN SI %	100 HR SI %
24	95.35	Fine sandy marl, massive/grumeleuse	SM/MG	1.0	0.2
24	95.40	Fine sandy marl, massive/grumeleuse	SM/MG	5.5	3+
24	102.80	Marl, strong, with very finely interstratified fine sandy marl, with grumeleuse structure from 103.0 m	MG (?)	2.0	0.5 (+)
POINT FIVE					
30	83.25	Thinly bedded marl, grumeleuse between 84.0 - 84.30. Core dinking 83.5 - 84.0 ('without doubt due to drilling')	MG	1.0	0.2
30	93.20	Marl, strong, tectonised 93.5 - 93.7	??	6	3.5 ++
30	104.20 (104 104.5)	Marl, laminated, weakly grumeleuse at the base of the unit; strong	N/MG ?	1.0	0.2
30	106.00	Marl, weakly grumeleuse or laminated, generally strong	N/MG?	1.8	0.2
30	110.70	Marly, weakly grumeleuse or laminated, generally strong	N/MG?	2.5	0.5+
30	118.70	Marl, with 'episodes un peu grumeleux', weak to medium strong	MG?	1.0	0.2
31	79.90	Marl, thinly bedded to laminated, strong	MG (=)	7.0	3.2 +
31	87.70	Marl, thinly bedded with microfissures, quite strong sensitive (1)	MG (??)	0/6	0.1
31	104.80	Marl, grumeleuse and locally thin bedded, weak sensitive (1)	MG	6	2.5 +
33	89.20	Marl, thinly bedded to laminated, fractured, sensitive	MG (=)	1.3	0.5 +
33	107.10	Marl grumeleuse, weak, sensitive	MG	1.6	0.4
36	86.40	Marl, thinly bedded, quite strong	M	1.1	0.4
36	93.40	Marl, quite grumeleuse, weak	MG (=)	5	2 ++

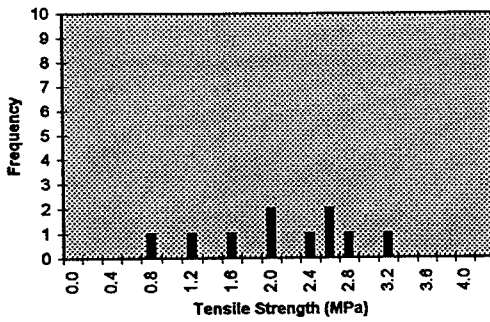
LEGEND CERN SI Specific Swelling Index for unloading Stress Change 100 kN/m² - 10 kN/m² in % strain

100 HR SI Swelling index over 100 hours for 15 kN/m² in final cycle

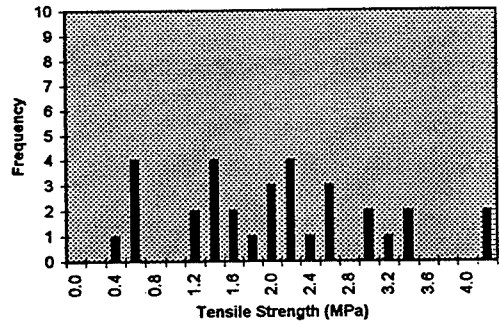
NOTES (1) Indicated significant ongoing swelling with time (++) indicates ongoing swelling with (+)



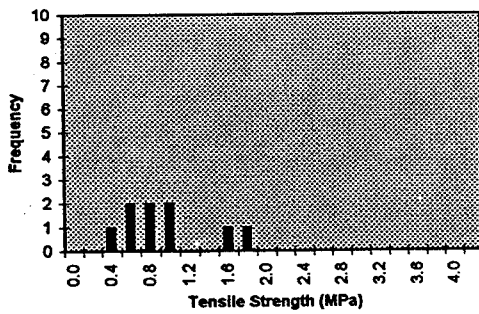
Frequency Distribution of Tensile Strength data for Intact Marl (PT 1 and PT 5)



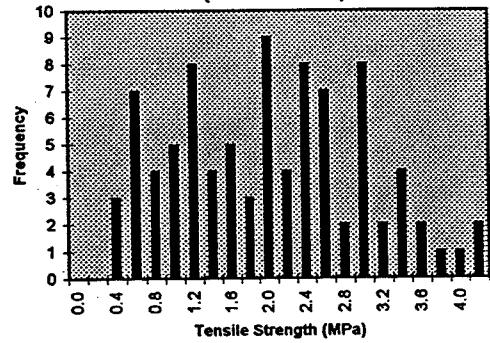
Frequency Distribution of Tensile Strength data for Sandstone (PT 1 and PT 5)



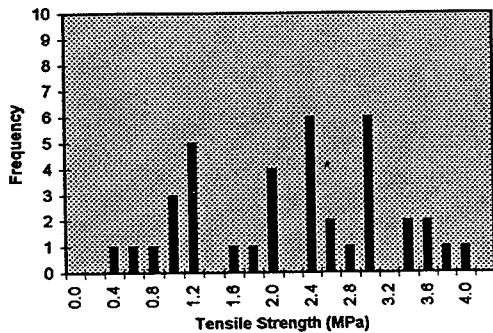
Frequency Distribution of Tensile Strength data for Marl Grumuleuse (PT 1 and PT 5)

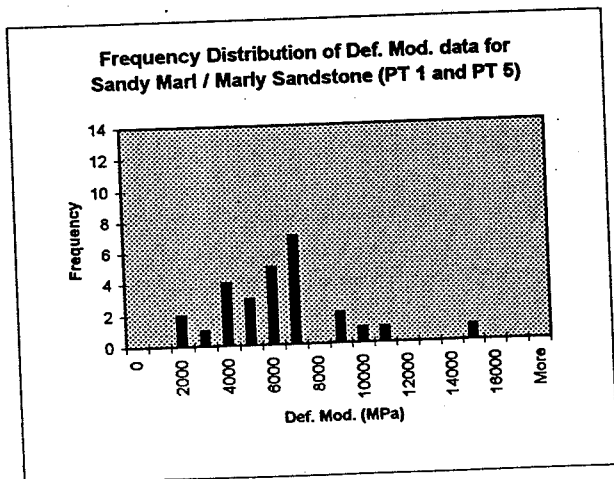
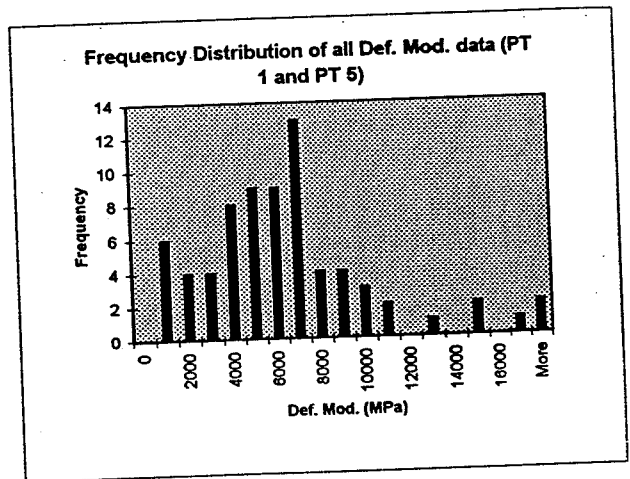
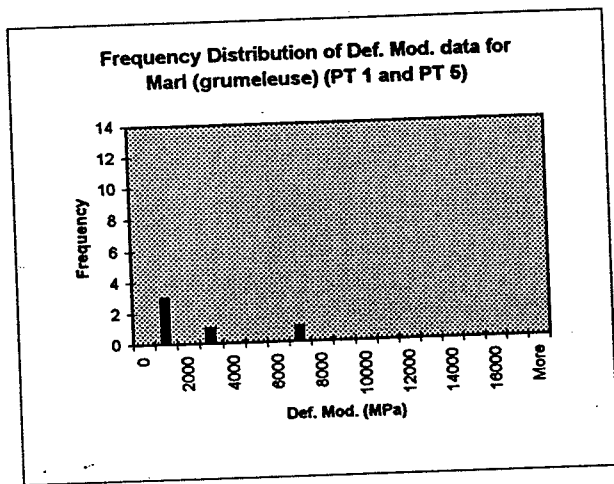
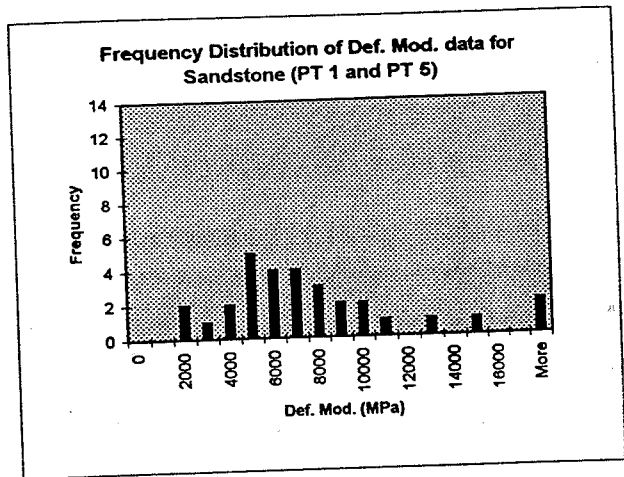
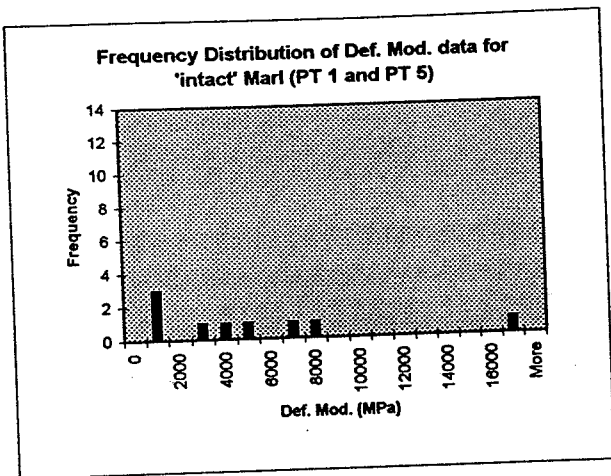


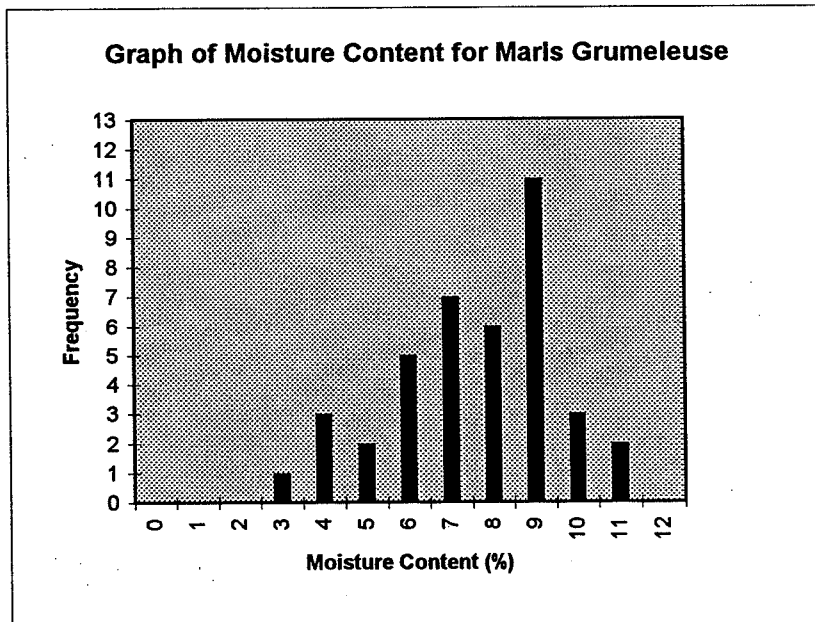
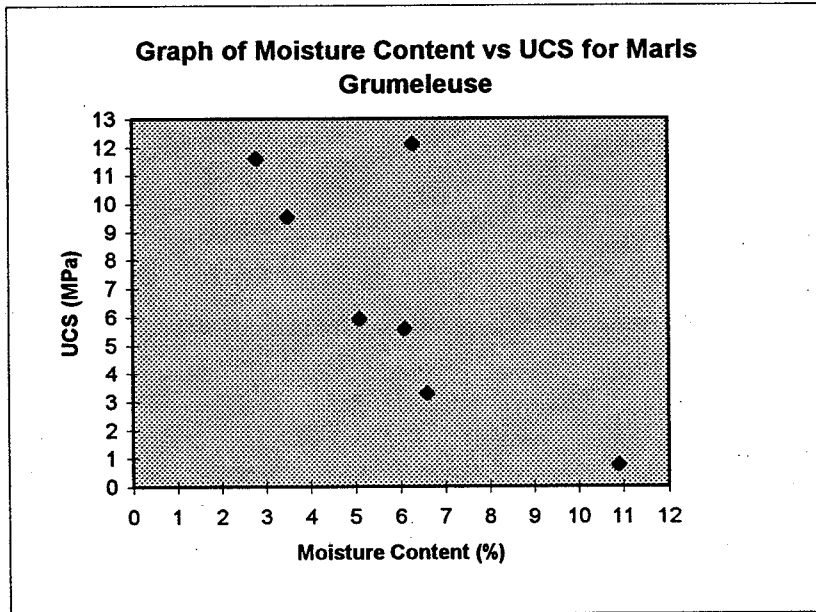
Frequency Distribution of all Tensile Strength data (PT 1 and PT 5)



Frequency Distribution of Tensile Strength data for Marly Sandstone/ Sandy Marl (PT 1 and PT 5)







GIBB



SGI INGENIERIE

CERN - LHC PROJECT- POINT 5

GRAPHS OF MOISTURE CONTENT AND UCS CHARACTERISTICS FOR MARL GRUMULEUSE

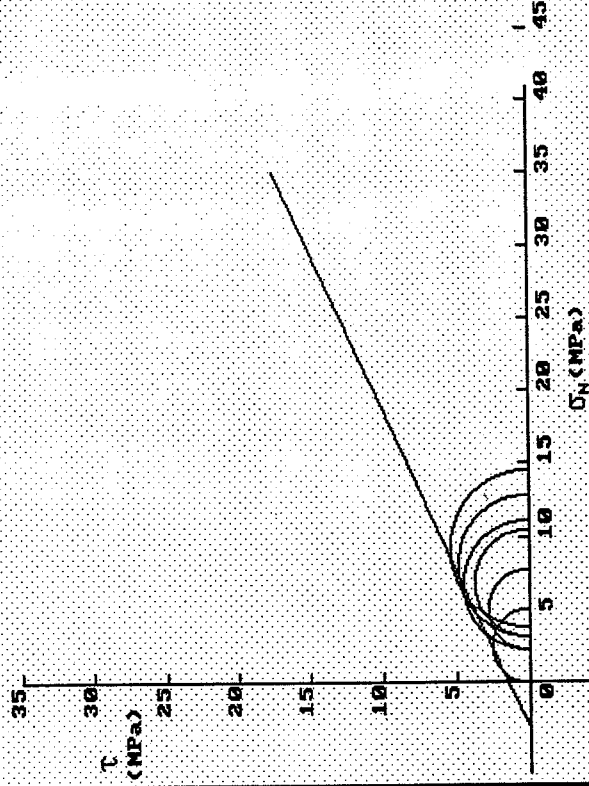
J96107A

Date
MAY 1996

Figure
9.4

FAILURE CRITERION FOR JOINTED ROCK MASSES

Mohr-Coulomb Envelope
for Triaxial Data
Marl Grumeleuse
Triaxial Tests - Peak Strength
Upper Bound Values
Intact Rock
— Fitted Curve



PARAMETERS

LINEAR REGRESSION ANALYSIS

$\phi = 24.58 \text{ deg}$
 $c = 1.494 \text{ MPa}$
 $\text{corr.} = 0.82857$

σ_3	σ_1
0.00	5.00
2.10	7.88
3.10	13.00
3.10	10.50
2.10	11.20
3.70	14.60

GIBB **GEOCONSULT**

SGI INGENIERIE

CERN - LHC PROJECT- POINT 5

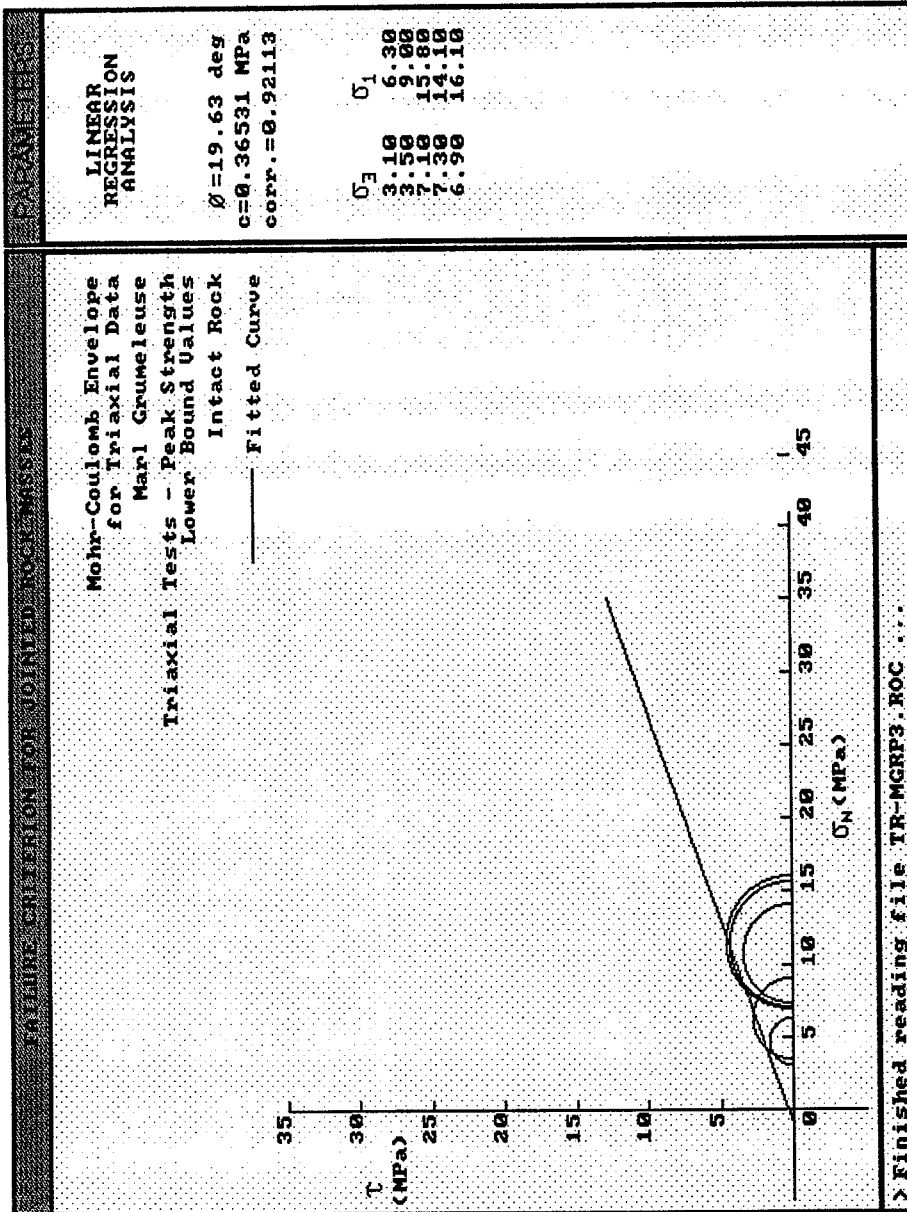
MOHR-COULOMB ENVELOPE FOR MARL GRUMULEUSE PEAK STRENGTH TRIAXIAL DATA (UPPER BOUND)

Date **MAY 1996**

Figure **9.5**

J96107A

PREPARE ENVELOPE FOR JOINTED ROCK MASSES



PARAMETERS
LINEAR
REGRESSION
ANALYSIS

$\phi = 19.63$ deg
 $c = 0.36531$ MPa
 $corr. = 0.92113$

σ_1	σ_3
3.10	6.30
3.50	9.00
7.10	15.00
7.30	14.10
6.90	16.10

GIBB **GEOCONSULT**

SGI INGENIERIE

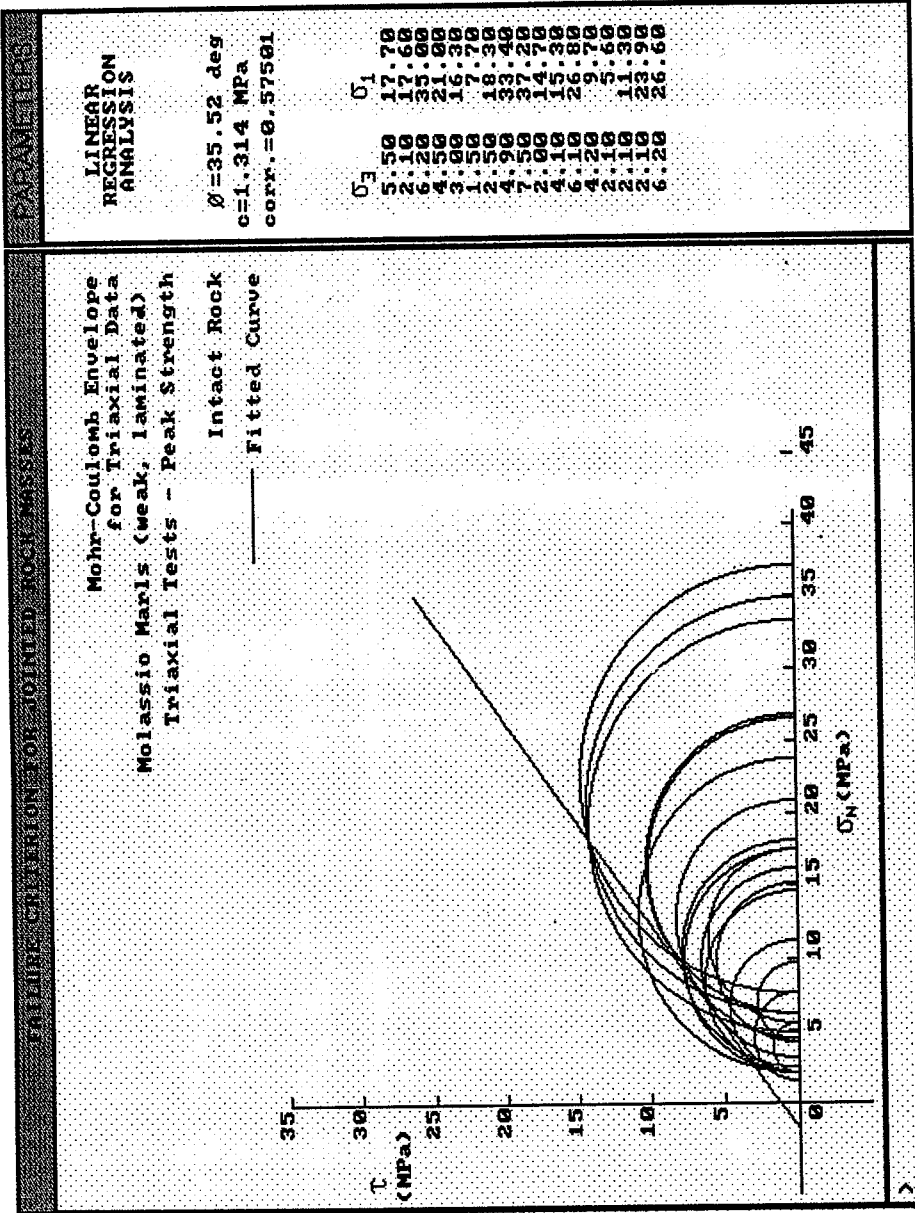
CERN - LHC PROJECT - POINT 5

MOHR-COULOMB ENVELOPE FOR MARL
GRUMULEUSE PEAK STRENGTH
TRIAxIAL DATA (LOWER BOUND)

J96107A

Date
MAY
1996

Figure
9.6



GIBB **GEOCONSULT**
SGE INGENIERIE

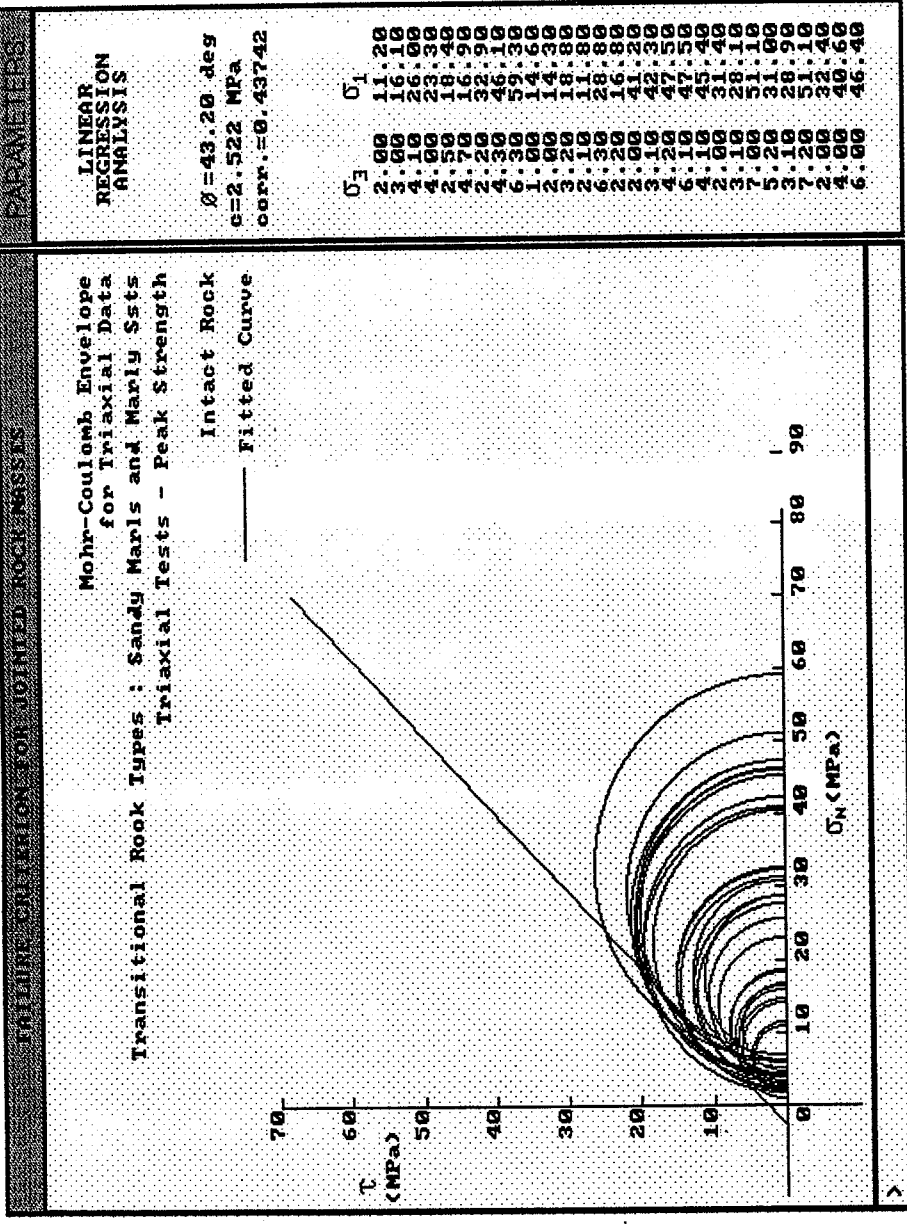
CERN - LHC PROJECT - POINT 5

MOHR-COULOMB ENVELOPE FOR
WEAK MARLS PEAK STRENGTH
TRIAxIAL DATA

Date
MAY
1996

Figure
9.7

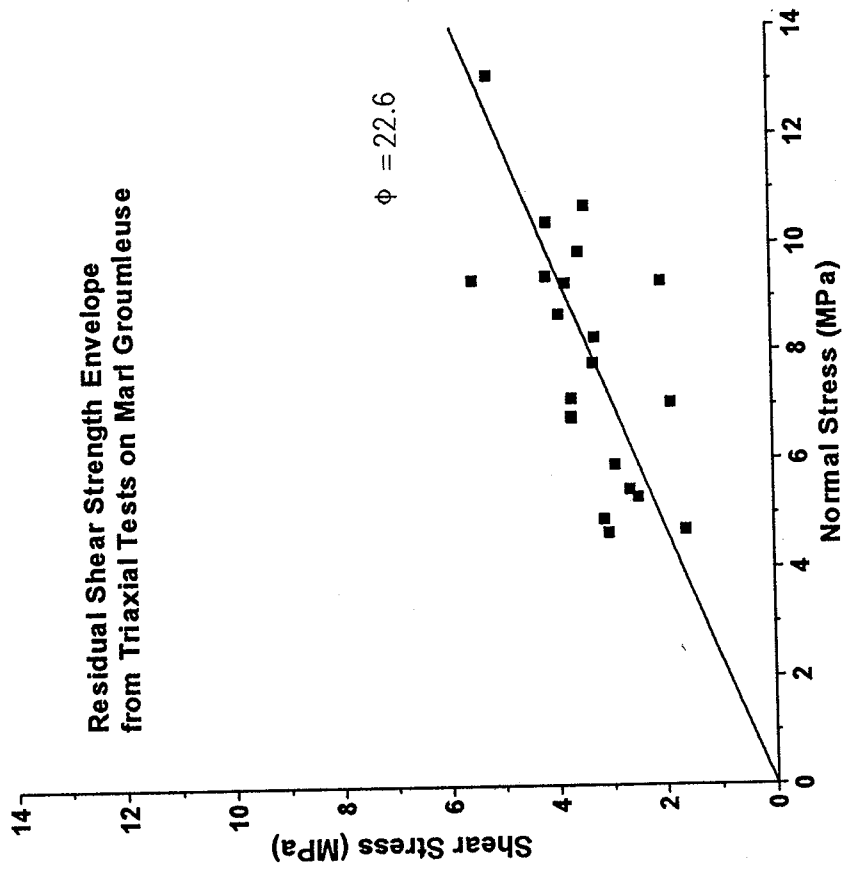
J96107A





CERN - LHC PROJECT- POINT 5
 MOHR-COULOMB ENVELOPE FOR
 TRANSITIONAL SANDSTONES
 AND MARLS PEAK STRENGTH
 TRIAXIAL DATA

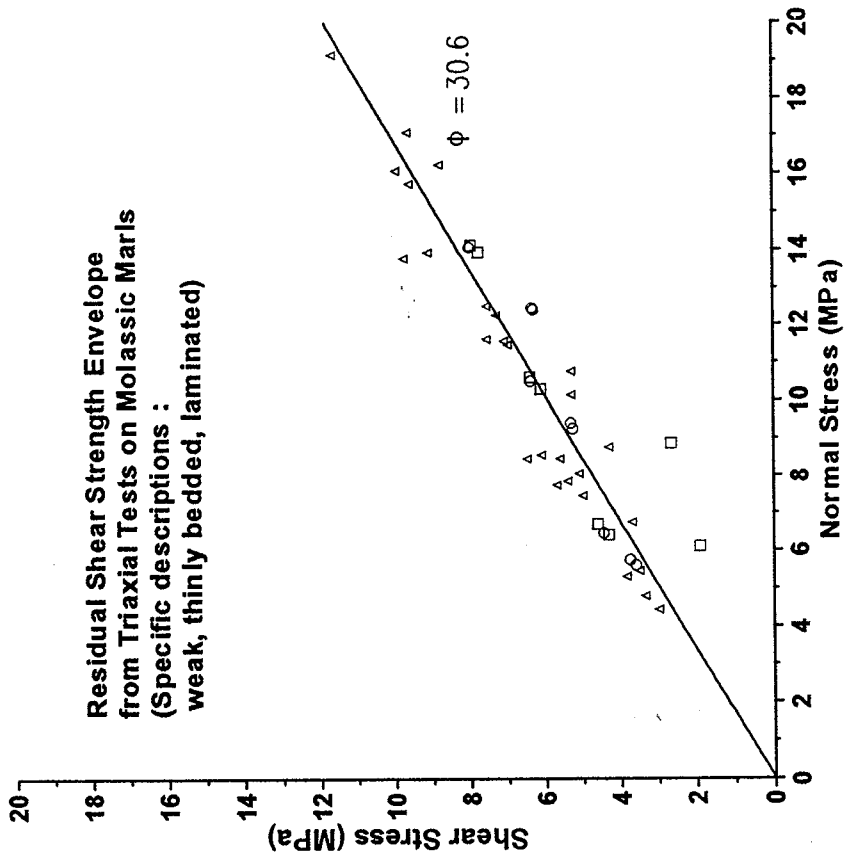
Date MAY 1996
 Figure 9.8

J96107A



GIBB  SEI INGENIERIE		CERN - LHC PROJECT- POINT 5		J96107A
		MOHR-COULOMB ENVELOPE FOR MARL GRUMLEUSE RESIDUAL STRENGTH TRIAXIAL DATA		Date MAY 1996

Residual Shear Strength Envelope
 from Triaxial Tests on Molassic Marls
 (Specific descriptions :
 weak, thinly bedded, laminated)



CERN - LHC PROJECT- POINT 5

MOHR-COULOMB ENVELOPE FOR MARL
 RESIDUAL STRENGTH TRIAXIAL DATA

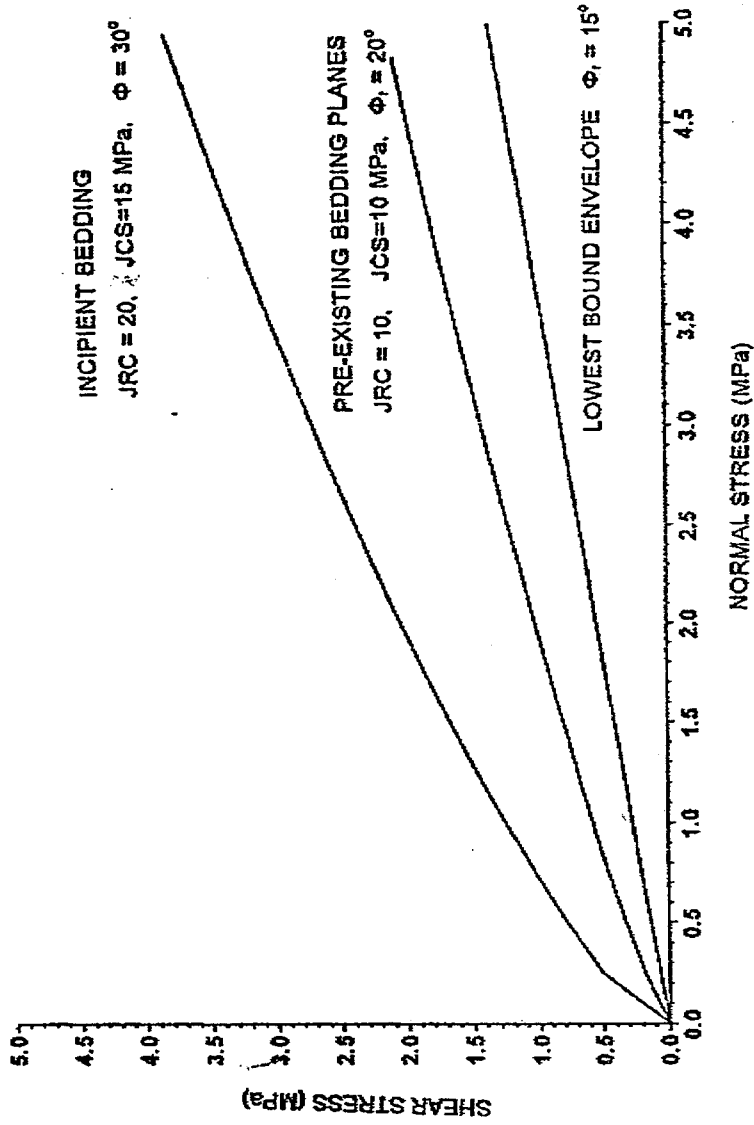
J96107A

Date

MAY
1996

Figure

9.10



CERN - LHC PROJECT- POINT 5
 BARTON-BANDIS ENVELOPES FOR
 EXISTING AND INCIDENT
 BEDDING DISCONTINUITIES

J96107A

Date
 MAY
 1996

Figure
 9.11

10. IN SITU STRESS

10.1 Introduction

Prior to the LHC investigation, it is understood that no in situ stress measurements had been undertaken in the Geneva area. In the design of caverns for the LEP project, a range of in situ stress conditions were modelled, and cavern responses predicted. Back analysis indicated horizontal-vertical stress ratios greater than one (Laughton 1988). From a consideration of topographic and geological constraints, the following inferences may be made concerning the in situ stress field:-

due to the large original thickness of molasse sediments high vertical and horizontal stresses will have accumulated.

- subsequent subaerial erosion of some 2000 m (Jenny et al 1995) will have relieved vertical stresses significantly.
- successive episodes of glaciation will have imposed vertical and horizontal stresses but during retreat of ice-sheets and associated erosion, vertical stresses will have been reduced
- the region is still tectonically active, due to the final phases of the Alpine orogeny (See Section 3.4).
- due to the limited relief of the basin, one principal stress is likely to be vertical.

From considerations of these factors, therefore, it is likely that horizontal stress magnitudes may be greater than the vertical stress magnitude, and that the vertical stress may be the minor principal stress.

10.2 LHC Hydrofracture Stress Measurements

During the LHC investigation, hydrofracture stress measurements (HFSM) were carried out at Points One and Five, by Plankel, Petzl & Partner and are reported in Annexe A8 of the Factual Report (GADZ 1996a).

The following results were obtained:

1. Out of a total of 22 HFMSMs and one test on a pre-existing fracture, only 4 tests yielded reliable data, amenable to analysis. This was due to the generation of horizontal fractures in the majority of tests, indicating that the minor principal stress is vertical.
2. The most reliable test results from Point Five indicates a σ_{hmin} value of 3.95 ± 0.15 MPa, and a σ_{hmax} value of 5.3 ± 0.7 MPa. However, there is a greater level of uncertainty associated with the latter value, inherent in the analysis of the HFMSM technique in weak rocks. These values are somewhat lower than those obtained at Point One, where the molasse formation extends almost to surface.
3. The orientation of the limited number of induced vertical fractures at Point Five indicates a σ_{Hmax} direction of NNE-SSW, compared with a direction of ENE-WSW obtained at Point One. However, the general NE to SW trend appears to have been demonstrated, and is consistent with shallow stress measurements undertaken at a site some 50 km to the Southwest.
4. Insufficient stress magnitude data were acquired to determine the complete in situ stress magnitude profile with depth. However, it is considered likely that extrapolations of the horizontal stress magnitude intercept the surface at non-zero compressive stresses (GADZ 1996a).

These conclusions generally confirm the inferences regarding the in situ stress field drawn from consideration of the geological setting. However, the conclusions appear to conflict with fault plane solutions from seismic events in the region (pers. comm G.Amberger) which indicate WNW-ESE compressive stresses, consistent with Alpine trends. It should be remembered, however, that it would not be unreasonable for in situ stress orientations within the basement seismogenic zone at depth to differ from orientations at comparatively very shallow depths.

The data generally suggest that horizontal stress magnitudes are of a similar order, which would give rise to the variation in induced fracture orientations. Furthermore, the ratio of horizontal to vertical stress magnitude is likely to lie within the range 1.2 to 1.8. Such uncertainties may be investigated by a number of parametric sensitivity analyses.

11. ADDITIONAL INVESTIGATIONS

From the assessment and interpretation of the existing ground investigation data, it can be seen that uncertainties remain in the following areas:

1. Orientation, spacing and persistence of sub-vertical discontinuity sets within the molasse. In addition, no orientation information is available for inclined discontinuities encountered and logged in the core.
2. The datasets used to determine rock material strength and deformability parameters are limited in size, and additional testing is desirable to ensure appropriate confidence in the detailed design. Such testing should incorporate measures to ensure close control of moisture contents, particularly for the marl grumeleuse units.
3. There is limited borehole coverage, in terms of area, for the surface structures. Further information on the distribution and nature of the moraine deposits is required, so that correlation's can be achieved across the complete site, and reliable, safe foundation designs can be prepared for the sites of major structures.
4. The amount of geotechnical data for the moraine deposits for the Point Five site is very limited. For the reliable and economic design of large shafts, it would be desirable to have additional, site specific, quantitative data concerning the composition, strength and deformability of the moraine deposits.
5. Whilst swelling test data have been acquired to provide an indication of the time and moisture content dependant behaviour of the marls, further useful data concerning the behaviour of the rock mass as a whole could be gained. In particular, in view of the localised problems occurring in two of the LEP caverns, an assessment could be made of existing loads conditions within the final concrete cavern lining. This would potentially benefit all LHC works and would potentially enable secondary lining design to be programmed with greater economy.

It is proposed therefore, that additional investigation works are undertaken as follows:

1. Discontinuity Orientation and Occurrence/Characteristics of Sub-Vertical Features.
During the main phase of the LHC investigation, a borehole television system was run in two boreholes to attempt to determine the orientation of inclined discontinuities within marl units. However, these features were associated with enlargements of the boreholes, and the fractures could not be observed in the borehole wall. It would therefore appear unlikely that application of BHTV or similar techniques would be successful, unless the borehole wall could be maintained in a good condition. Borehole stability could be enhanced by such measures as drilling with heavy mud, together with the use of additives to inhibit the swelling of clays. Alternative geophysical imaging techniques, such as orientated resistivity logging, where pads of electrodes are in physical contact with the borehole wall, may prove more successful.

It is unlikely that any of the LHC boreholes (if they were not grouted on completion) would remain in a suitable condition for further geophysical logging. It is recommended therefore, that consideration be given to drilling additional cored boreholes, the core from which should be logged in detail. In order to sample subvertical features, inclined or core drilling could be undertaken, either from surface or from existing underground excavations at the Point Five site. An inclined borehole from surface would need to be some 140 m in length (at 60 degree inclination) to provide data at the depth of interest. Shorter holes could obviously be drilled from existing Point Five excavations. Such work would also provide samples for additional laboratory testing. It should be noted that resistivity based geophysical techniques cannot be applied in horizontal or dry boreholes.

As an alternative to additional drilling work, it is recommended that detailed logging, including discontinuity logging, of core from horizontal boreholes currently being drilled should be undertaken. This would provide a general indication of the possible occurrence of sub-vertical features. In addition, further laboratory testing, comprising direct shear tests, of any sub-vertical discontinuities should be undertaken to provide strength and deformability characteristics for these features. A minimum of ten tests is recommended. The database for strength and deformability of other discontinuities is also limited and further testing, particularly of discontinuities within the marl grumeleuse could usefully be undertaken. An additional five tests are recommended.

2. Additional Laboratory Testing of Marl Grumeleuse Material.

This should comprise multistage triaxial testing at 100 mm diameter, with careful control of moisture contents, to limit moisture dependant strength variations. In addition, the confining stress range should be considered in relation to the likely stress induced by the proposed works. Samples should preferably be retrieved from the Point Five site, although it would be possible to use samples of marl grumeleuse from boreholes currently being undertaken, with slightly less confidence. A minimum of ten additional tests should be carried out.

3. Additional Investigation within the Moraine.

In order to provide complete coverage of the sites of major surface structures, it is recommended that an additional two boreholes should be drilled from the surface at the Point Five site. This will allow the geological correlation of moraine deposits to be extended across the complete site, and enable additional laboratory and in situ testing to be carried out. Additional data would then be available to enhance confidence in foundation designs. This would also provide further data for shaft design.

The boreholes should be at least 220 mm in diameter, and should be sampled continuously to provide both undisturbed U100 samples from cohesive deposits, and large bulk samples from granular deposits. A large number of Standard Penetration Tests should also be carried out, generally at 1.0 m centres, to provide a reliable design database. It is envisaged that the boreholes would not exceed 30 m in depth.

In addition, the foundation conditions at the sites of individual shallow pad foundations should be investigated by trial pits, logged by an engineering geologist.

4. Time-Dependant Rock Mass Behaviour.

Overcoring stress measurement could be carried out with existing cavern linings to determine the magnitudes and orientations of stresses within the lining. With a knowledge of the primary support system, it is probable that a number of inferences concerning time-dependant rock mass behaviour could be made, which will enable designs to be developed with more confidence. It is estimated that up to three overcoring tests in each of three locations should provide sufficient data. Triaxial overcoring cells or USBM deformation gauges should be used.

REFERENCES

Amberger G 1971. Geologie du Canton de Geneve. Publications de la Societe Suisse de Mecanique des Sols et des Roches. No. 82 1971.

BS5930: 1981. Code of Practice for Site Investigation BSI 1981

Charollais, J & Badonx, H 1990. Suisse Lemannique, Pays de Gevieve et Chablais Guide Geologiques Regionaux. Masson 1990

CIRIA Report 143, 1995. The Standard Penetration Test (SPI): Methods and Use. Construction Industry Research and Information Association. London. 1995.

EUROSAT 1982. Etudes Structurale par radar monte sur satellite et avion dans la zone du piemont du Jura, entre Thoiry et Gex (ain) a l'aplom du Projet LEP du CERN. Report reference EUROSAT/CA/jb/8929. September 1982.

Freeze R. A. & Cherry J. A. 1979. Groundwater. Prentice - Hall 1979.

GADZ 1993 CERN PROJECT LHC. Synthese Geologique et Geotechnique. Geotechnique Appliqué P & C Deriaz & CIE SA 1993.

GADZ 1996a. CERN PROJECT LHC - LOT2. Reconnaissances Geologiques et Geotechniques. Geotechnique Appliqué P & C Deriaz & CIE SA 1996.

GADZ 1996b. CERN PROJECT LHC - LOT2. Reconnaissances Geologiques et Geotechniques. Rapport d'Interpretation. Report No. 3545/92 1996.

GADZ 1982a. Project LEP - Secteur Plaine. Sondage SPL 5.4. Rapport Geologique et Geotechnique. Report No. 2271/39 1982.

GADZ 1982b. Project LEP - Secteur Plaine, Sondages SPL 5.7 et 5.8. Rapport Geologique et Geotechnique. Report No. 2271/41 1982.

GADZ 1982c. Project LEP - Secteur Plaine, Sondages SPL 5.6 et 5.10. Rapport Geologique et Geotechnique. Report No. 2271/49 1982.

GADZ 1995 Project LHC Point 5. Sondage SLHC 14 et 15. Report No. 3543/7 1985.

Jenny, J., Burri, J. P., Muralt, R., Pugin, A., Schegg, R., Ungemach, P., Unataz, F. D., and Wernli, R. 1995. Le forage geothermique de Thonex (Canton de Geneve): Aspects stratigraphiques, techtoniques, diagenetiques, geophysiques et hydrogeologiques. Eclogae geol. Helv. Vol 88 No. 2 pp 365 - 396, 1995.

Laughton, C. 1988. Excavation & support of the CERN point 4 experimental zone.

Peck, R. B. Hanson, W. E. & Thornburn, T. H. 1974. Foundation Engineering. 2nd Ed. John Wiley and Sons. New York 1974.

Service Cantonal de Geologic. Isohypes du Contract Molasse Quaternaire. Echelle 1:25,000.

CERN/964, 1996 CERN, Project LHC, Point 5, Essais De Tracage. Universite De Liege, Laboratoires De Geologie De L'Ingenieur, D'Hydrogelogie et De Prospection Geophysique. Issued 27/6/96.

APPENDIX A

DERIVATION OF GEOMECHANICAL PARAMETERS OF THE ROCK

1 INTRODUCTION

The derivation of the geomechanical parameters of the molasse rock types was based on the following:

- a) The general appreciation of ground conditions in terms of anticipated behaviour and primary stability mechanisms within the particular rock types and the underground complex development.
- b) The analytical requirements in terms of key behavioural models.
- c) The available data base of laboratory test results.

Key characteristics of the molasse rock mass are the stratified, bedded and overall weak nature of the rock components. As in all weak, stratified rock masses, shear overstress along bedding is the primary stability mechanism. Overstress of weak component materials may also occur in the crown and invert zones (interactively controlled by structure and induced stress) or may develop peripherally depending on the prevailing stress-to-strength analogy.

The following sections contain explanations as deemed appropriate for clarity on the derivation of the geomechanical parameters for the key geotechnical units.

2 KEY GEOTECHNICAL UNITS - ROCK MASS COMPONENTS

The key geotechnical units in the stratified sequence were described as follows:

- Marl (laminated)
- Sandstone ('weak' to 'strong')
- Sandy marl/Marly sandstone ('transitional' materials)
- Marl grumeleuse (collectively encompassing weak, thinly bedded, tectonised marls).

Bedding contacts separating different lithologies can be termed generally as discontinuities. Due to the very low tensile strength along such contacts, it is prudent to allow for the discrete nature of such features and the associated directional shearing implications upon stability.

Such discontinuity bedding partings are described in the main report. Shear strength parameters were derived separately for the various types of interfaces due to the differences in intrinsic characteristics such as the angle of basic friction and the material uniaxial compressive strength. Weakest structural features were those associated with the grumeleuse marl intercalations.

Incipient bedding and associated strength anisotropy was also considered as a feature of potential importance in controlling the strength of the laminated and thinly bedded members of the rock mass. Incipient bedding was inferred to represent a ubiquitous structure.

3. DATA BASE OF LABORATORY TEST RESULTS

The following sources of laboratory test data were reviewed:

1. Synthèse Géologique et Géotechnique: Report 574/5
Géotechnique Appliquée P. & C. Deriaz & CIE. S.A., 22 Juillet 1993 JFH/vb.
2. CERN-LHC Essais de Laboratoire, Report R377, Mars 1996.
Ecole Polytechnique Fédérale de Lausanne, Département de Génie Civil - Institut des Sols, Roches et Fondations, Lab, de Mécanique des Roches.

The tests comprised:

- uniaxial compression tests
- direct shear tests
- triaxial tests
- swelling tests

4. MODELS OF MECHANICAL BEHAVIOUR

4.1 Rock Materials

All intact rock units were modelled as Mohr-Coulomb materials. The model was considered as appropriate for the case representing fundamental shear failure mechanism. Such a failure mode is considered relevant for the present rock types given the low strength, compressible nature and the expected low to non-dilatant behaviour under high deviatoric stresses in the volume immediately surrounding the caverns.

The c , ϕ parameters for all geotechnical units were derived from the evaluation of the triaxial test data.

4.2 Structure

Parameters required to describe the shear strength and stiffness behaviour of the modelled discontinuities were derived according to two models of shear behaviour:

- a) The linear Mohr - Coulomb model
- b) The non-linear Barton - Bandis model

The latter has the advantage of simulating stress- and displacement-dependent dilatant shear behaviour, also allowing for scale effects. For the purposes of numerical simulation, the B-B model can also be applied to derive M-C model stiffness parameters at the stress levels of relevance.

The required parameters for B-B model shear behaviour characterisation were derived mostly by expert judgement and limited core observations.

Values of c , ϕ parameters, were derived from the direct shear tests parallel to pre-existing bedding and incipient bedding. For the grumeleuse marl interfaces data from both triaxial and direct shear tests were evaluated.

5. DERIVATION OF GEOMECHANICAL PARAMETERS

5.1 Basic Rock Material Parameters (Table 9.4)

The parameters were derived from all data on UCS, E and ν from the pre-1993 and the recent LHC investigations.

The value $\sigma_c = 5$ MPa for the grumeleuse marl corresponds to the typical range of moisture contents according to the histogram in Figure 9.1 (for $w = 6-9\%$) the corresponding $\sigma_c = 2-5$ MPa). The value appears to represent the upper bound estimate for the typical range of moisture contents. However, the sensitivity of such materials to moisture changes (drying), sampling disturbance, etc. on the measured properties should not be overlooked.

In conclusion, a lower value of 2-3 MPa could be suggested as a conservative estimate to waive uncertainty, until further factual documentation becomes available.

5.2 Triaxial Strength of Materials (Table 9.5)

The derivation of the c , ϕ parameters (peak and residual) is discussed in the main text. The derived parameters generally agree with those obtained from an overall review of the test data recently presented in the following report:

- Reconnaissances Geologiques et Geotechniques - Rapport d'Interpretation
No. 3545/92, June 1996 JFH/fd
GEOTECHNIQUE APPLIQUEE P. & C. DERIAZ & CIE SA (GADZ 1996b).

The comparison between the derived parameters is self - explanatory.

Rock Type	Peak		Residual c=0	
	c (MPa)	ϕ (°)	ϕ_r (°)	
Marly Sandstone GADZ 1996b		4.2	39.6	40
	GIR	6.9	33.8	41
Marl (laminated - thinly bedded) GADZ 1996b		1.8	35.6	36
	GIR	1.3	35	35
Marl Grumeleuse GADZ 1996b		0.9	20.1	23.6
	GIR	0.95	22.2	22

5.3 Strength Parameters of Geotechnical Units (Table 9.6)

Those were derived by regression analyses of the available data grouped to the key geotechnical units.

5.4 Shear Strength Parameters for Discontinuities

5.4.1 Pre-existing (open) bedding (Table 9.7)

The values were derived from linear regression of the direct shear tests results (reverse/forward cycle - multistage testing).

The overall average residual angle corresponds to the mean of 6 values at the start of axes during the 3 forward and 3 reverse cycles.

The lowest bound values were obtained from the last two values recorded at the end of the last reverse and forward cycles.

5.4.2 Incipient bedding (Table 9.8)

The above clarifications should be referred to.